NMDAr BLOCKING BY MK801 ALTERS HIPPOCAMPAL AND PREFRONTAL CORTEX OSCILLATIONS AND IMPAIRS SPATIAL WORKING MEMORY IN MICE.

P. Abad-Perez[1,2]; L. Martínez-Otero[2], V. Borrell[2]; R. Redondo[3], J.R. Brotons-Mas*[1,2]

[1] Universidad Cardenal Herrera CEU, Elche

[2] Instituto de Neurociencias UMH-CSIC. Alicante

[3] Roche Pharma Research and Early Development, Neuroscience and Rare Diseases, Roche Innovation Center Basel

*Corresponding author

Jorge R Brotons-Mas

e-mail: Jorge.brotonsmas@uchceu.es

Address: Universidad CEU Cardenal Herrera; Plaza Reyes Católicos, 19. 03204 Elche – Alicante, Spain

Instituto de Neurociencias UMH-CSIC; Avd Ramón y Cajal SN, Edificio Ramón y Cajal, 03550,San Juan de Alicante, Alicante, Spain.

Tel. +34965426486

Declaration of interest

The authors declare that they have no known competing financial interests or personal relationships that could have appeared to influence the work reported in this paper.

Abstract

Abnormal NMDAr function has been linked to rhythmopathies, psychosis, and cognitive dysfunction in schizophrenia (SCZ). Here, we investigate the role of NMDAr hypofunction in pathological oscillations and behavior. We implanted mice with tetrodes in the dorsal hippocampus and medial prefrontal cortex (mPFC), administered the NMDAr antagonist MK801, and recorded oscillations during spontaneous exploration in an open field and in the y-maze spatial working memory test. Our results show that NMDAr blockade increased locomotor activity, impaired spatial working memory, and disrupted the correlation between oscillations and speed of movement, crucial for internal representations of distance. In the hippocampus, MK801 increased gamma oscillations and disrupted theta/gamma coupling, while in the mPFC, it increased the power of theta and gamma, and generated high-frequency oscillations (HFO 155-185 Hz), also disrupting theta/gamma coupling. Spatial working memory tests in the y-maze revealed that theta/gamma coupling was consistently higher in correct trials after MK801 administration but were lower in the baseline condition. Theta/gamma co-modulation mediated by NMDAr function might be essential to explaining several of SCZ's cognitive symptoms and might be crucial to explain hippocampal-PFC interaction.

Keywords: Schizophrenia, oscillatory activity, hippocampus, prefrontal cortex, NMDAr.

Significance Statement:

NMDAr hypofunction might be at the bases of cognitive symptoms and oscillopathies found in Schizophrenia. In this work we aimed to understand further this link. We found that NMDAr hypofunction altered theta/gamma co-modulation in the hippocampus and the PFC explaining spatial working memory deficits.

Introduction

Schizophrenia is a disabling disorder characterized by negative, positive, and cognitive symptoms, e.g., lack of social interest, psychosis, working memory deficits (Owen et al., 2016). A dominant theory about SCZ's etiology is the dopaminergic hypothesis, which posits that the disorder is caused by dopamine imbalance and is supported by the therapeutic effects of anti-dopaminergic drugs (Meltzer and Stahl, 1976; Ban, 2007). However, neuroleptic medications fail to treat negative and cognitive symptoms, suggesting that multiple mechanisms are at play in the generation of schizophrenia's symptoms (Bowie and Harvey, 2006; Kirkpatrick et al., 2006; James et al., 2018). The NMDAr hypofunction hypothesis of SCZ may offer a complementary explanation of the etiology of this disorder, including its cognitive symptoms. NMDAr antagonists can induce schizophrenia-like symptoms in patients and healthy subjects (Malhotra et al., 1997; Adler et al., 1998). Schizophrenic patients showed a reduced expression of NMDAr in the dorsolateral prefrontal cortex (DLPFC), a brain region strongly involved in working memory and executive function, impaired in SCZ (Beneyto and Meador-Woodruff, 2008; Weickert et al., 2013). NMDAr hypofunction seems to dysregulate dopamine levels (indirectly increasing striatal dopamine levels), linking NMDAr function with the previously observed dopamine imbalance (Wędzony et al., 1993; Vollenweider et al., 2000; Del Arco et al., 2008). Additionally, animal models of SCZ based on NMDAr hypofunction successfully mimic the positive, negative, and cognitive symptoms as well as structural brain changes observed in schizophrenic patients (Olney et al., 1999; Eyjolfsson et al., 2006; Abekawa et al., 2007; Adell et al., 2012; Jodo, 2013; Murueta-Goyena et al., 2017). Finally, the pharmacological blockade of NMDAr produces not only cognitive symptoms like those seen in SCZ but also its associated aberrant oscillatory activity and interneuron dysfunction (Hertzman et al., 1990; Kristiansen et al., 2006; Hakami et al., 2009).

The deletion of NMDAr from parvalbumin-positive interneurons (PV^+) in rodent models triggers cognitive symptoms recapitulating many of those observed in SCZ (Weickert et al., 2000; Belforte et al., 2010; Korotkova et al., 2010; Mena et al., 2016). Dizolcipine, or MK801, is an NMDAr antagonist that non-competitively blocks NMDAr's voltage-dependent ion channels (Huettner and Bean, 1988). It is commonly used as a model of SCZ in rodents as it reproduces its cognitive deficits, gamma power alterations, and the emergence of high-frequency oscillations (HFO) across different brain regions. At the cellular level, NMDAr hypofunction induced by MK801 administration reduces the firing of GABAergic interneurons, which in return increases the firing rate of excitatory pyramidal neurons (Jackson et al., 2004; Homayoun and Moghaddam, 2007). Taking all this evidence together, it is possible to suggest that the NMDAr hypofunction hypothesis offers a possible mechanism that links the cognitive deficits, the aberrant oscillatory activity, and the interneuron dysfunction observed in SCZ, while at least partially explaining some of the dopamine changes typically observed in patients (Uhlhaas and Singer, 2010; Lewis et al., 2012; Moghaddam and Javitt, 2012).

Despite the accumulation of data regarding the role of NMDAr hypofunction at the level of cellular and synaptic mechanisms, its relationship to cognition remains poorly understood. Here, we aimed to understand how NMDAr blockade by MK801 can affect oscillatory activity, behavior, cognition, and the dialog between the dorsal and intermediate CA1 hippocampal region and the prefrontal cortex (PFC). These hippocampal regions are connected directly and indirectly with the PFC (Hoover & Vertes, 2007), and their interaction is critical for executive function and SCZ (Jones and Wilson, 2005; Sigurdsson and Duvarci, 2016). We were especially interested in determining the oscillatory correlates involved in spatial cognition and decision-making in spatial working memory. For this reason, we recorded simultaneously from the intermediate CA1 and the PFC and investigated the effect of MK801-mediated NMDAr blockade in oscillatory activity, behavior, and spatial working memory performance. We

expected to find changes in the gamma band and distortion of the hippocampus/PFC interaction associated with working memory deficits. Our results were coherent with these predictions. In addition, NMDAr blockade, generated area-specific oscillatory changes in the hippocampus and the PFC and altered the relationship between oscillatory activity and motor behavior.

Methods

Subjects

Male wild-type mice C57, N=9, age p60 to p90 supplied by the UMH “Servicio de Experimentación Animal (SEA)" were used. Mice were maintained on a 12 h light/dark cycle with food and water available *ad libitum* and were individually housed after electrode implantation. Our procedures were approved by the UMH-CSIC ethics committee, and the regional government and met local and European guidelines for animal experimentation (86/609/EEC).

In vivo recordings on freely moving mice

Microdrives, (Axona ltd) mounting four tetrodes (12 µm tungsten wire, California Fine Wire Company, Grover Beach, CA, USA) were implanted under isoflurane anesthesia (1.5%) while buprenorphine (0.05mg/kg, s.c.) was supplied as analgesia. Craniotomies were performed above the hippocampus and medial prefrontal cortex (mPFC), targeting the hippocampal CA1 region (AP: -2-2.5, M-L: 1.2 V: 0.6 mm) as well as the prelimbic region of the mPFC (AP: 1-2, M-L:0.5-1, V: 1.2-1.9 mm).

Data acquisition.

Electrophysiological recordings were obtained using a 16-channel headstage (Axona Ltd, UK). (gain x1), with an infrared light-emitting diode (LED) to track mouse position (Brotons-Mas et al., 2010; Brotons-Mas et al., 2017; del Pino et al., 2013). Signals were amplified (400 to 1000x), bandpass filtered (0.3 Hz to 24 kHz, DacqUSB system, Axona, UK) and recorded at 48 kHz/24-bit precision. For Local field potential recordings (LFP), tetrodes were lowered to reach specific stereotaxic coordinates in the mPFC. Unit activity, ripples (high-frequency events 150-200Hz), and theta power were used as electrophysiological landmarks to determine electrode location in the CA1 pyramidal layer. Once tetrodes were in the target areas, we started the recording protocols.

Power spectrum analysis

Local field potentials were analyzed using custom-written MatLab codes (Mathworks, Natick, MA, USA). Raw recordings were FIR filtered (<1.2 kHz) and downsampled to 2.4 kHz, as in previous work (Del Pino et al., 2017). Data obtained in open field recordings was used to characterize oscillatory activity. Running speed was computed based on the animal's position. Epochs of behavior in which the speed of movement was above 5 cm/s were included for analysis. In this way, we obtained similar behavioral episodes across the different conditions. Spectral power was calculated (in decibels 10log10) using the Thomson multi-taper method included in Chronux signal processing toolbox(Bokil et al., 2010). The spectrogram was plotted to visualize the power spectrum in the time domain notch filter (50 Hz and 100 Hz) was implemented to eliminate electrical noise. Also, high-frequency noise (135-145 Hz) associated with chewing artifacts and some motor behaviors were observed in the periodogram. Therefore, we did not include for analysis this band, and we eliminated it from the periodogram plots. The functional connectivity between the hippocampus and the prefrontal cortex was measured by calculating frequency coherence. This measurement describes the degree of co-occurrence of different frequencies in the activity recorded across different areas.

To establish the correlation between oscillatory activity and movement speed, we segmented the signal in non-overlapping windows of 1 s. Then, we calculated the power spectrum and obtained the theta (4-12Hz) / delta(<3.9Hz) ratio to eliminate epochs contaminated by mechanical artifacts. Then we investigated different oscillatory bands for the resulting epochs their correlation with the speed of movement. We calculated the power spectrum for theta type I (6.5-12Hz), linked to motor behavior. Also, we obtained the power values for low (30-65 Hz) and high gamma (66-130 Hz) bands. Also, we calculated theta and gamma activity power for epochs in which locomotor activity was not present, speed <5 cm/s. Then, to control for volume propagation in the PFC, we performed a bipolar derivation, subtracting the signal obtained from two channels in different tetrodes implanted in the PFC and we performed the same LFP analysis previously described.

Gamma modulation index (GMI)

The gamma modulation index was calculated as previously described (Korotkova et al., 2010). In brief, the raw LFP was filtered in the theta band (4-12 Hz) and in different higher frequency intervals: low gamma (30-65 Hz), high gamma (66-130), and high-frequency oscillations (155-185 Hz). The gamma and HFO envelopes were then calculated to determine the power of the signal across the different theta cycles; the

maximum and minimum values were used to calculate the gamma index of modulation (GMI).

$$GMI=(max-min)/(max+min).$$

Also, hippocampal theta/ PFC gamma bands co-modulation was calculated to measure region interaction using the same procedure.

Drug administration and dose

Before drug administration, a baseline recording was obtained. This condition served to calculate ratios of LFP power to determine change due to drug administration controlling for possible electrode position drifting across days. After baseline recordings, mice were injected subcutaneously with MK801 (0.075 mg/kg) or with the vehicle solution. Recordings were initiated at the peak of drug bioavailability, 15 min after injection. Drugs were administered following a counterbalanced scheme across alternate days, spacing the recordings at least 48h.

Behavioral Protocol

Recordings were performed in the animal's home cages for several minutes to ensure that the electrodes were placed in the CA1 pyramidal layer. Recordings were then implemented during spontaneous exploration in an open field of 50 x 50 cm. The animals were subsequently left to rest for five minutes in their home cage before 8 minutes of y-maze testing. After the last y-maze trial, mice were recorded in their home cage. The drug or vehicle was administered, and the process started again.

Working memory in the y-maze

We used the y-maze to measure working memory. This test is a reliable approach for cognitive testing and provides a measurement of spatial working memory based on the ethology of mice (Miedel et al., 2017). Testing was carried out on a transparent Y-shaped maze (40 x 10 cm per arm). Mice were placed at the end of the central arm and allowed to explore the maze for 8 minutes. The sequence of arm entries was obtained from the x,y position coordinates and automatically analyzed using custom-made scripts in MATLAB. Correct alternations were those in which the animal went into an arm not visited recently, e.g., correct visit sequence: arm 1-2-3. We considered incorrect alternations when animals repeated the same arm in a sequence of trials, e.g. arm 1-2-1. The final score was calculated as the percentage of correct triads using the formula below:

$$\text{Spontaneous alternation } \% = \frac{\#\ spontaneous\ alternations}{total\ number\ of\ arm\ entries - 2} \times 100$$

We searched for different electrophysiological biomarkers of spatial working memory to investigate normal and pathological mechanisms during memory performance in the y-maze. To this end, we analyzed LFP epochs of 1s duration, half a second before the mice entered the decision area of the y-maze (the central triangle between the three arms) and half a second later. We only included experiments consisting of at least nine entries, ensuring the sampling of a minimum of LFP epochs. Finally, we included five animals in the vehicle condition and seven in the MK801 experiments. As animals explored much less in the vehicle condition, we centered our analysis on the baseline vs. MK801 conditions, focusing on the LFP obtained in these sets of experiments and including a final N=7 mice.

Anatomical verification of electrode location

After completing experiments, animals were deeply anesthetized using sodium pentobarbital (Euthanasol, 1 mL／kg, i.p.) and transcardially perfused with saline and 4% paraformaldehyde; the brains were removed, sliced in 40 µm sections, and prepared for Immunohistochemistry against DAPI, NeuN (Merck,ltd) and GFAP (Adigene technologies) for electrode localization.

Statistical analysis

Distribution of variables was tested for normality using Kolmogorov-Smirnov test. To determine statistically significant differences, parametric and non-parametric tests were used. ANOVA repeated measures was used for normally distributed variables and Greenhouse-Geisser correction applied when sphericity criteria were not met. This correction allows for a more conservative interpretation of the results after adjusting the degrees of freedom. Partial eta squared (η^2) was calculated as an estimation of the size effect and the statistical power reported. The Friedman test was used for non-normally distributed variables. Then, paired comparisons between specific conditions were tested using t-test for repeated measures and non-parametric Wilcoxon test when appropriate. In the case of correlations analysis normality was verified and the parametric Pearson coefficient and the associated Student's t-test were calculated. All descriptive values were expressed as mean ± the standard error (S.E.). Statistical significance was set at $p < 0.05$, and Bonferroni corrections were used when necessary. All statistical analysis was performed using SPSS (IBM, V27) software package.

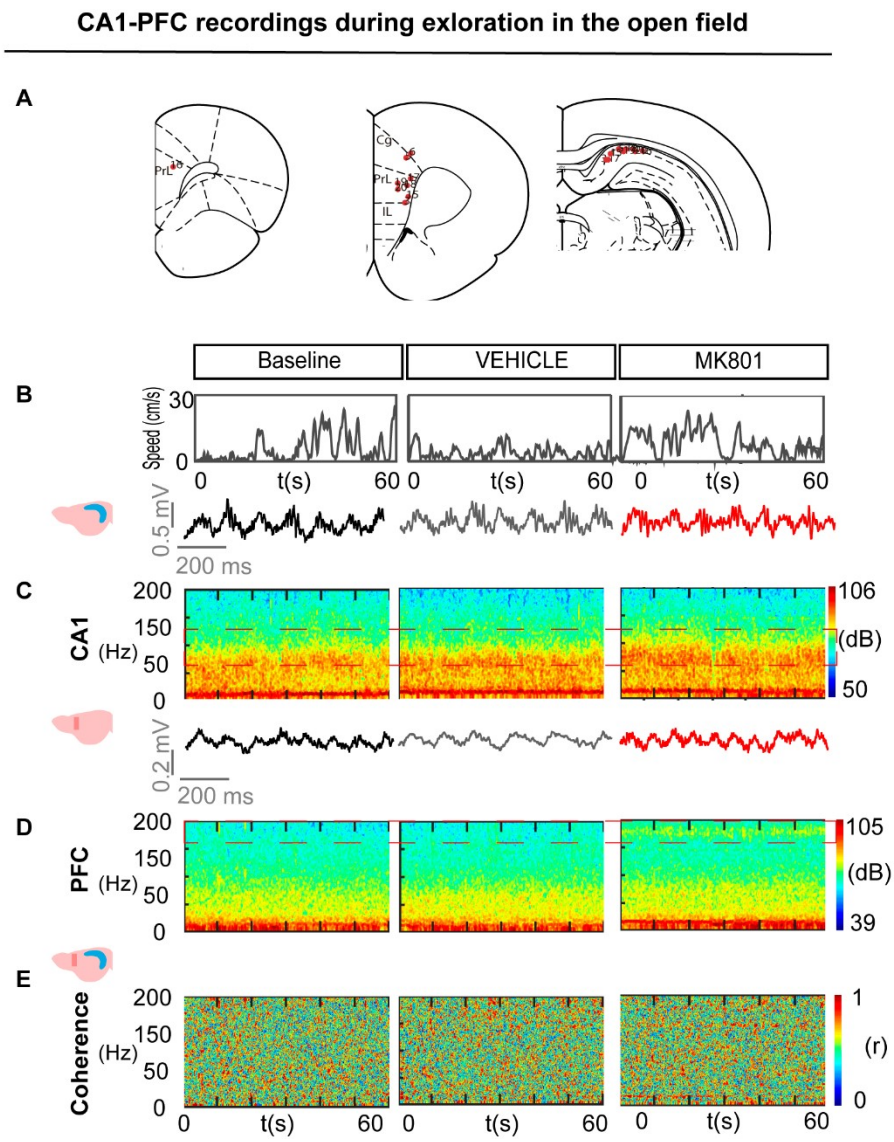

Figure 1. Freely moving recordings. A. Anatomical reconstruction of electrode implant location in the intermediate hippocampus and the PFC. Recordings were performed during freely moving exploration in an open field and during the y-maze experiment. Sessions consisted of a 900s baseline recording followed by a second recording performed after the administration of vehicle or MK801. The position and the speed of movement were monitored. Low-frequency artifacts, such as physical bumping against the open field wall, were eliminated by calculating the theta/delta ratio. Also, a notch filter for 50hz and the harmonic 100 Hz were implemented. Dual implants in the HPC and the PFC, tend to generate a high-frequency noise (135-145 Hz) associated with chewing artifacts and some motor behaviors. For this reason, this specific band was eliminated from the analysis. B. Representative speed of movement during recordings. C and D. Representative recordings in CA1 and the PFC during different conditions and their corresponding spectrograms. E. Representative coherence hit maps. Note the increase in gamma activity in CA1 and the presence of HFO 155-185 Hz in the prefrontal cortex, (red squares) as well as the increase in speed during the MK801 condition.

Results

Behavioral effects of MK801

We investigated exploratory activity by comparing the speed of movement, the total distance run, the percentage of immobility time, and the latency to visit the center of the arena. We found significant differences in all four variables. (*speed,* $f_{(1,11)=}$ 66.296, $p<0.0001$, $\eta^2=0.892$, $\beta=1$; *total distance,* $f_{(3,24)=}$ 43.371, $p<0.0001$; $\eta^2=0.844$, $\beta=1$; *% of immobility time,* $f_{(3,24)=}$ 51.226, $p<0.0001$, $\eta^2=0.865$, $\beta=1$; *latency*, $\chi2_{(3)}=10.950$, $p=0.012$, *Friedman test*). Then we aimed to determine the specific conditions in which these variables were significantly different. First, we found that animals presented higher levels of activity during the baseline vs. the vehicle condition. This was proved true for the speed of movement, total distance run, immobility time and latency, however this last parameter did not reach significance after Bonferroni correction ($p=0.0125$), (*baseline vs. vehicle, speed (m/s),* 0.04±0.006 vs. 0.03±0.004; $t_{(8)}= 4.39$, $p=0.0019$, *distance (m),* 45.22±7.5 vs. 30.51±11.4; $t_{(8)}= 3.39$, $p=0.008$; *% time*, 48.32±64.45; $t_{(8)}= -5.5.3$, $p=0.001$; *baseline vs. vehicle, time (s),* 83.84±51.7 vs. 213.2±62.5, $z=-2.1$, $p=0.036$, *Wilcoxon test*), see Fig 2. This difference might be accounted for by order effect and the habituation to the testing apparatus etc. Then, we sought to evaluate whether significant changes in locomotor behavior were produced after NMDAr blockade finding significant differences in all variables (*speed (m/s),* 0.04±0.003 vs. 0.11±0.009; $t_{(8)}= -8.6$, $p=0.0001$; *distance (m)*, 47.1±7.5 vs.. 107.6±5.4; $t_{(8)}= -6.918$, $p=0.0009$*; % time*, 49.03±4.11 vs.. 13.39±2.15; $t_{(8)}= 5.972$, $p=0.0009$, *baseline vs.. mk801,* 87.49±47.98 vs. 17.18±8.51, $z=-1.955$, $p=0.01$, *Wilcoxon test*). Then we looked for further differences between equivalent conditions. First we verified that mice behaved in a consistent manner across days in the baseline condition (*speed,* $t_{(8)}= 1.010$, $p=0.342$; *distance (m)*, $t_{(8)}= -0.418$, $p=0.687$*;immobility,* $t_{(8)}= -0.247$ $p=0.8$; *Latency*, $z=-0.296$, $p=0.767$, *Wilcoxon test*). Then to account for order effects and to determine if MK801 had a significant effect we compared the vehicle vs. MK801 conditions, finding significant differences in speed, total distance, immobility time, and latency (*speed,* $t_{(8)}= -8.9$, $p=0.0001$; *distance,* $t_{(8)}= -7.19$, $p=0.001$; *immobility* , $t_{(8)}= -9.19$, $p=0.0001$; *latency* , $z=2.521$, $p=0.012$, *Wilcoxon test*). All significant differences were maintained after Bonferroni corrections ($p<0.0125$); see Fig 2E.

NMDAr blocking by MK801 administration reliably increased locomotor activity in mice during open field spontaneous exploration, while no significant differences were found

between both baseline conditions for any of the variables indicating a consistent behavior across days for the baseline experiments.

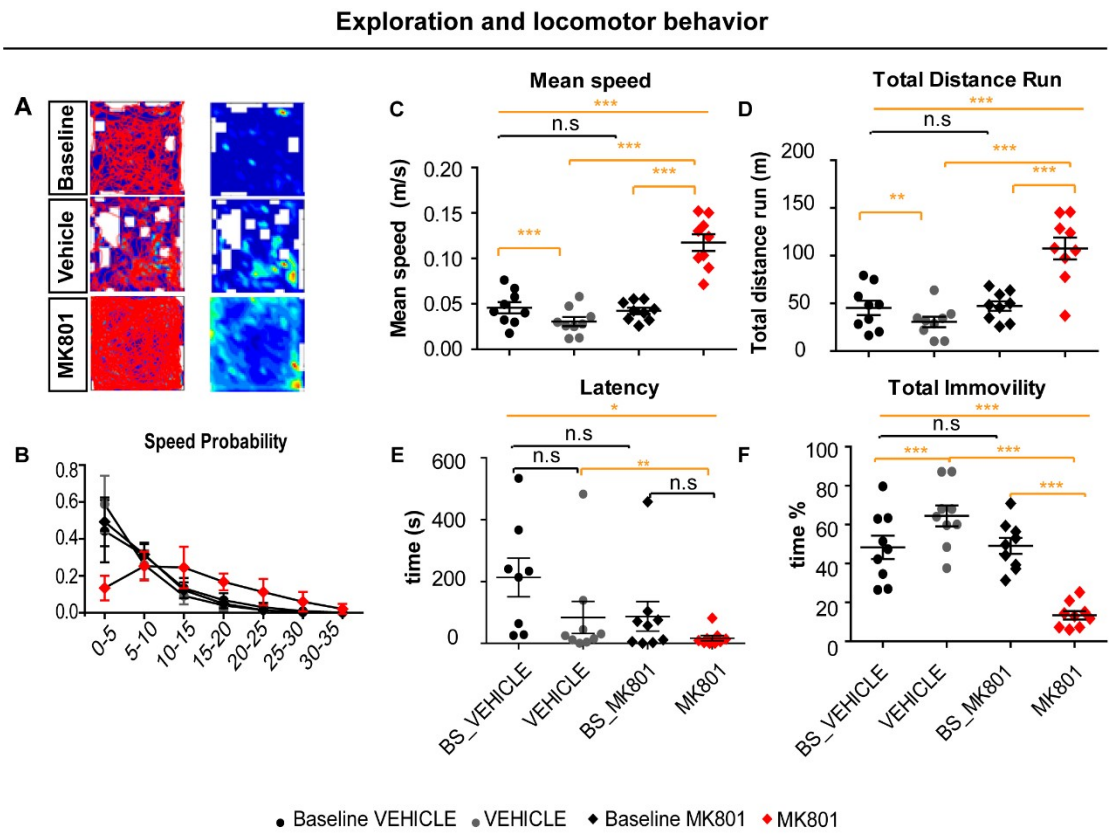

Figure 2. MK801 increased exploration and locomotor behavior. A. Representative tracking and dwelling time maps for the baseline, vehicle, and drug conditions. Red color indicates bins with the highest level of occupancy. B. Probability of speed occurrence in the different conditions. MK801 administration produced a reduction of low speeds and an increase of higher speeds probability. C. Mean speed was reduced during the vehicle condition and increased after MK801 administration. D. Total distance run was augmented during the MK801 condition. E. Latency to visit the center of the open field, only 8 points are displayed as one of the animals never visited the center. F. Total immobility. Note that the behavior across days in the baseline conditions was very similar indicating the existence of behavioral consistency across days for similar experimental conditions.

MK801 impaired spatial working memory in the y-maze.

We aimed to determine if cognition was affected during NMDAr blockade. For this reason, we implemented the y-maze, a behavioral test based on the tendency of mice to alternate visits to different locations. As we had different group size due to inclusion criteria, see methods, in the y-maze, (baseline vehicle and vehicle n=5, baseline MK801 and MK801, n=7) we decided to perform pairwise comparisons between specific conditions, *baseline vehicle vs. vehicle, baseline MK801 vs. MK801*. First, we investigated the activity of mice in the y-maze in the baseline vehicle vs. vehicle conditions observing changes in exploratory behavior characterized by a reduction of exploration during the vehicle experiment as demonstrated by the mean speed of movement, total distance run, immobility and by the decreased number of y-maze arm entries (*m/s,* 0.052±0.005 vs. 0.028±0.003; $t_{(4)}$= 3.48, p=0.025, *distance (m);* 31.01 ±2.8 vs. 17.23±1.82; $t_{(4)}$= 3.4, p=0.026; immobility % , 40.36±6.16 vs. 64.9±4.8; $t_{(4)}$= -3.102, p=0.036; *entries* 25±3.4 vs. 14±2.1; z=-1.06, p=0.0109), see Fig 3. Significance was not maintained after Bonferroni corrections (p=0.025), except for the number of entries.

When we analyzed the MK801 baseline vs. the MK801 condition, we observed changes in speed of movement, total distance, no changes in the immobility time but an increase in the total number of y-maze arm entries (*m/s,* 0.037±0.005 vs. 0.07±0.01; $t_{(6)}$= -3.883, p=0.008; *distance (m),* 23.49 ±8.5 vs. 38.02±4.9; $t_{(6)}$= -3.209, p=0.018; immobility %*,* 57.22 ±6.3vs. 38.9±7.3; $t_{(6)}$= -2.378, p=0.055; *entries* 17±5.7 vs. 39.2±6.3, z=2.366, p=0.018). Significant changes were maintained after Bonferroni corrections (p=0.025).

To measure working memory, we evaluated the animals' tendency to alternate between different arms of the y-maze. The final score was calculated as the percentage of correct triads performed, see methods and figure 3. We observed no significant change in performance in the baseline vs. the vehicle condition (*% of alternation,* 59.08±7.9 vs. 57.34±9.2; $t_{(4)}$= 0.125, p=0.907.). On the other hand NMDAr blockade, clearly reduced performance in the y-maze (*% of alternation,* 62.58±4.8 vs. 37.38±2.56; $t_{(6)}$= 4, p=0.007), see Fig 3F.

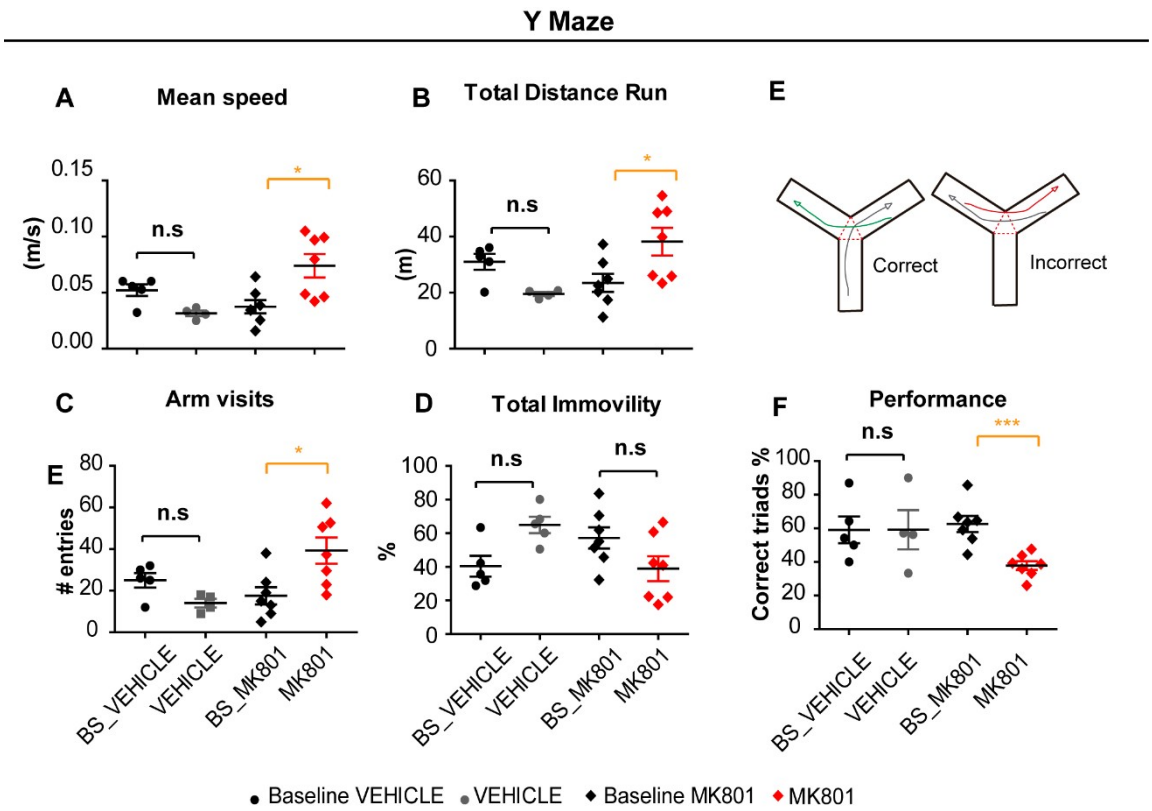

Figure 3. MK801 impaired spatial working memory. A. Mean speed was reduced during the vehicle condition vs. its baseline in a not significant manner after Bonferroni corrections. On the other hand, MK801 administration significantly increased mean speed values. This trend was similar for the total distance run and the immobility times, although this last did not reach statistical significance C and D. E. Examples of correct and incorrect trials. F. Lower performance in the y-maze revealed a deficit in spatial working memory after NMDAr blockade.

Effect of MK801 on CA1 oscillations during spontaneous exploration

We investigated how MK801 affected hippocampal and PFC oscillations and the dialogue between these areas. Oscillatory activity is modulated by the behavioral state, especially the subject's locomotor behavior (Kramis et al., 1975; Long et al., 2014). We first investigated if this relationship was maintained across conditions. To carry out this analysis, we segmented the signal in non-overlapping windows of one second of

duration and calculated the power spectrum and speed movement, comparing them across the different conditions.

First, we looked at theta oscillatory activity. As expected, we could observe that lower theta frequencies, theta type II 4-6-4 Hz, displayed a low correlation with the speed of movement (data not showed). For this reason, we considered for analysis theta type I, 6.5-12Hz, normally related to voluntary motor behaviors and the speed of movement (Kramis et al., 1975). We included only animals in which the speed of movement indicated a significant correlation across the four investigated conditions (n=6). Normally, animals did not showed speeds higher that 25 cm/s, except in the MK801 condition, see fig 2B, 3A, 4A, therefore, to eliminate a possible ceiling effect in the power vs. speed relationship, we only included epochs in which the speed was between 0 to 25 cm/s. First, we observed a possible difference for hippocampal theta/speed correlations across conditions indicating a higher correlation during the vehicle condition and lower during the MK801. However this data trend was not significant ($f_{(1,15)}$= 3.087, p=0.59, η^2=0.382, β=0.6). Also, we investigated the relationship between low gamma (30-65Hz) and high gamma (65-120Hz). This analysis revealed a low correlation between low gamma and the speed of movement, see figure 4B. However, higher gamma oscillatory activity was strongly modulated by the speed of movement. We found significant differences between conditions ($\chi^2_{(3)}$=13.533, p=0.004, *Friedman test).* Post-hoc test, showed that high gamma/speed correlation was significantly higher during the vehicle condition when compared with its baseline (*baseline vs. vehicle, r),*0.52±0.03 vs. 0.59±0.011; $t_{(8)}$= -3.179, p=0.013). On the other hand, this correlation was significantly decreased when we compared MK801 with its baseline (*baseline vs. MK801, (r),* 0.55±0.03 vs. 0.37±0.05; z=-2.547, p=0.01, *Wilcoxon*). This difference was also observed between the vehicle and the MK801 condition ($t_{(8)}$= 5.598, p=0.0005). All these comparisons were significant after Bonferroni corrections.

Thus, NMDAr blocking by MK801 altered the relationship between CA1 oscillatory activity and speed of movement, especially affecting the high gamma band (66-130Hz).

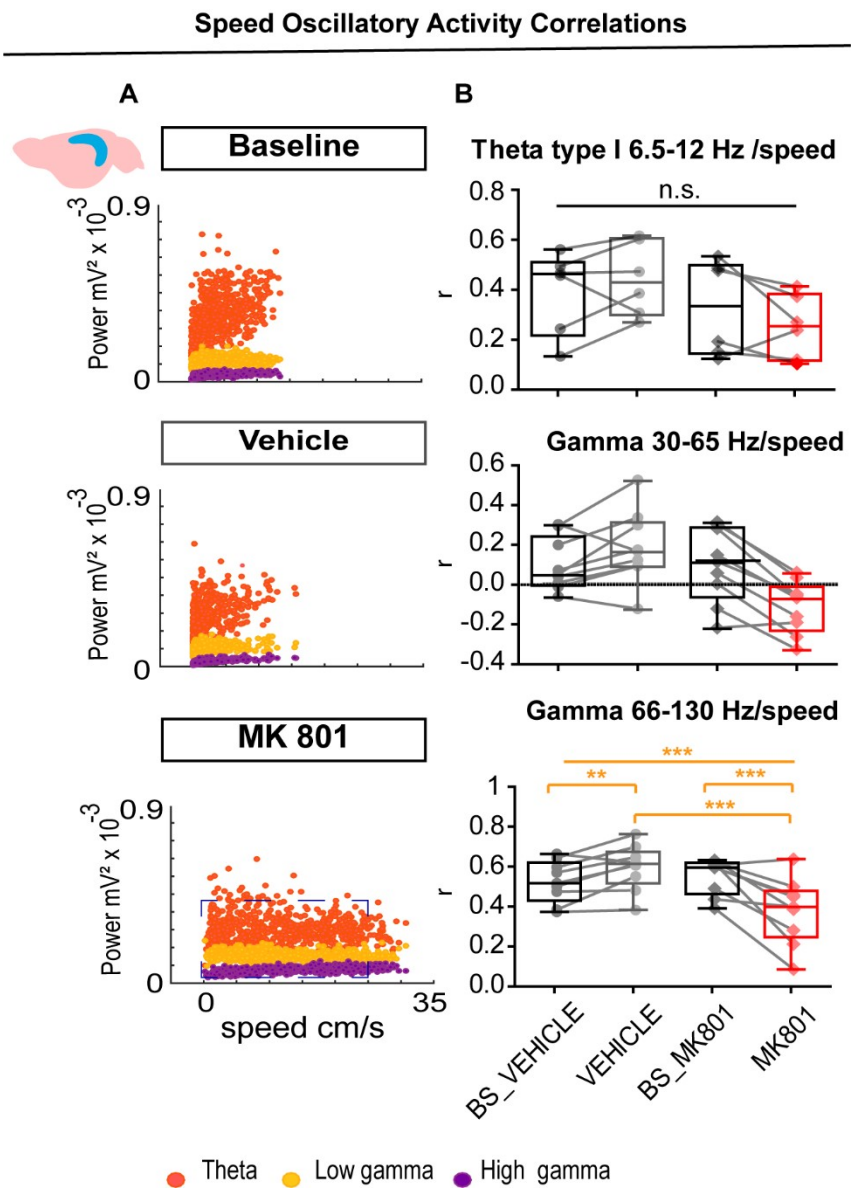

Figure 4. MK801 administration disrupted the relationship between hippocampal oscillatory activity, and the speed of movement. A. Representative scatter plots for one animal across baseline, vehicle and MK801 condition. Each dot represents mean values for power and the speeds of movement, see color code. B. Mean correlation values between theta type I (6.5-12HZ), low gamma and high gamma with the speed of movement. Analysis of theta correlations only included animals showing significant correlations, (n=6). Low gamma presented poor correlation with the speed of movement and no statistical test was performed. High gamma presented a robust correlation with the speed of movement (n=9). Results indicated that theta /speed correlation decreased in a non-significant manner after MK801 administration. High gamma showed a similar trend to theta, showing a significant increase in the vehicle condition and a reduction during the MK801 experiment.

Effect of MK801 on CA1 and PFC oscillatory activity.

To control for behavioral states as a potential confounding variable influencing oscillatory activity, we calculated the power spectrum for the entire recording session over different time windows (see Fig 1 for representative recordings and Fig 4 for results). Then, we selected epochs of behavior in which the speed of movement was above 5 cm/s during at least > 2 sec, therefore analyzing epochs that considered similar exploratory behaviors.

First, we looked to oscillatory activity in the CA1 region across conditions. We observed significant differences only for the high gamma band (delta, $f_{(1,8)}$= 1.253, p=0.298; η^2=0.135, β=0.2; theta, $f_{(1,8)}$= 0.219, p=0.7, η^2=0.027, β=0.1; alpha, $f_{(1,8)}$= 0.569 p=0.492; η^2=0.066, β=0.1; beta, $\chi2_{(3)}$=6.0, p=0.108; low gamma, $\chi2_{(3)}$=5.93, p=0.115; high gamma, $\chi2_{(3)}$=14.6, p=0.002; *HFO,* $\chi2_{(3)}$=3.53, p=0.316), see fig 5A, 5A´and 5C. We aimed to determine if the observed difference in the high gamma band was due to MK801 administration. For this, considering the known results and the distribution of values, we performed pairwise comparison between the vehicle condition vs. the MK801 and the baseline MK801 vs. the MK801 condition. We found that high gamma activity was significantly increased after MK801 administration (vehicle vs. MK801, mV^2, 0.00086±0.0.0001 vs. 0.0014±0.0.0002; z=-2.310, p=0.021, *Wilcoxon; baseline MK801 vs. MK,* mV^2, 0.0009±0.0.0002 vs. 0.0014±0.0.0002; z=-2.666, p=0.008, *Bonferroni correction for two comparisons p<0.025*). We completed this analysis in the CA1 LFP, looking at the power spectrum during epochs in which movement speed was below 5 cm/s. This allowed us to test for possible power spectral changes during non-exploratory behavior. In CA1, we found no significant changes in the power of theta neither in the baseline vs. vehicle nor baseline vs. MK801 (mV^2, 0.0035±0.0.0006 vs. 0.0036±0.0.0006; $t_{(8)}$=0.607, p=0.561; 0.0043±0.0.0003 vs.. 0.0003±0.0.0008 $t_{(8)}$=-1.022, p=0.337). When we looked at the low and high gamma band, we observed that these were significantly increased in the MK801 condition (mV^2, low gamma, 0.0014±0.0.0007 vs. 0.0019±0.0.0003; z=2.547, p=0.011; *high gamma*, 0.00061±0.0.0001 vs. 0.0011±0.0.0002; z=2.666, p=0.008, *Wilcoxon*). Therefore, changes due to MK801 were consistent with independence of the speed of movement.

Then, we looked to oscillatory activity in the PFC finding that significant differences for theta, alpha, high gamma and HFO, (delta, $\chi2_{(3)}$=3.533, p=0.316, *Friedman*; theta, $f_{(2,15)}$= 10.539, p=0.001, η^2=0.568, β=0.96; alpha, $f_{(1,12)}$= 4.956, p=0.034, η^2=0.383, β=0.632; beta, $f_{(3,24)}$= 2.791, p=0.062, η^2=0.259, β=0.6; low gamma, $\chi2_{(3)}$=4.62, p=0.204; high gamma, $\chi2_{(3)}$=8.067, p=0.045; *HFO,* $\chi2_{(3)}$=8.733, p=0.033), see fig 5B,

5B' and 5D. Then, we performed pairwise comparison to determine the effect of the different treatments on oscillatory activity. We found that theta activity was significantly higher in the MK801 condition vs. its baseline and when compared with the vehicle condition (*baseline vehicle vs. vehicle*, *mV²*, 0.0012±0.0.0002 vs. 0.0012±0.0.0001; $t_{(8)}$=-0.547 p=0.599; *baseline MK801 vs. MK801, mV²*, 0.0012±0.0.0002 vs. 0.002±0.0.0003; $t_{(8)}$=-3.931 p=0.004; *vehicle vs. MK801*; $t_{(8)}$=-3.837 p=0.005; *Bonferroni correction for three comparisons p<0.016*). We also found that alpha activity was significantly higher in the MK801 condition (*baseline vehicle vs. vehicle*, *mV²*, 0.000081±0.0.00001 vs. 0.000077±0.0.00001; $t_{(8)}$=0.964 p=0.364; *baseline MK801 vs. MK801, mV²*, 0.0000077±0.0.00001 vs. 0.00011±0.00003; $t_{(8)}$=-3.197 p=0.013; *vehicle vs. MK801*, $t_{(8)}$=-2.420 p=0.042; *Bonferroni correction for three comparisons p<0.016*). This significant difference was preserved only for MK801 baseline vs. MK801 condition after Bonferroni corrections. Similarly, high gamma activity was higher in the MK801 vs. its baseline condition, (*baseline vehicle vs. vehicle*, *mV²*, 0.00013±0.0.00003 vs. 0.00015±0.0.00003; z=-1.836, p=0.066; *baseline MK801 vs. MK801, mV²*, 0.00013±0.0.00003 vs. 0.00017±0.0.00005; z=-2.192, p=0.028; *vehicle vs. MK801*, z=-0.418, p=0.678; *Bonferroni correction for three comparisons p<0.016*), however this difference was not preserved after Bonferroni corrections. We also observed that HFO were higher in the MK801 vs. its baseline, (*baseline vehicle vs. vehicle*, *mV²*, 0.000032±0.0.000005 vs. 0.000044±0.0.00001; z=-0.770, p=0.441; *baseline MK801 vs. MK801, mV²*, 0.000026±0.0.000001 vs. 0.000061±0.0.00003; z=-2.310, p=0.021; *vehicle vs. MK801*; z=-1.481, p=0.139; *Bonferroni correction for three comparisons p<0.016*). Part of the recorded LFP in the PFC might be volume propagated. For this reason, we performed the same analysis after referencing the PFC signal to electrodes located in different tetrodes implanted in the PFC, see fig 6. We observed significant differences in the delta band ($\chi2_{(3)}$=10.333, p= 0.016, *Friedman*). Post-hoc test showed that this difference was due to a significant increase of delta power in the MK801 condition vs. its baseline (*vehicle vs. MK801, mV²,* 0.000091±0.0.00003 vs. 0.000016±0.0.00006; z=-2.547, p=0.011). Also, alpha and high gamma oscillations presented significant differences (alpha, $\chi2_{(3)}$=8.733 p=0.033; high gamma, $\chi2_{(3)}$=0.017, p=0.017, *Friedman*). These differences were explained by changes in the MK801 vs. the baseline condition (baseline *vs. MK801, alpha, mV²,* 0.00032±0.0.00001 vs. 0.00047±0.0.00002; z=-2.429, p=0.008, *Wilcoxon;* baseline *vs. gamma, MK801, mV²,* 0.000101±0.0.00003 vs. 0.00012±0.0.00004; z=-2.666, p=0.008, *Wilcoxon*). Theta, beta, low gamma activity and HFO seem not to be significantly different after Friedman non parametric test for repeated measures (theta, $\chi2_{(3)}$=7.267 p=0.064, beta,

$\chi 2_{(3)}$=1.40, p=0.0706, low gamma, $\chi 2_{(3)}$=4.467, p=0.215, *HFO,* $\chi 2_{(3)}$=0.68 p=0.068, *Friedman*).

Finally, we calculated the ratio of change in the different bands between the baseline/vehicle vs. baseline/MK801. First, we selected those bands in which scores were apparently different in the distribution, see figure 6I. Significant changes in the CA1 were found between 3-9 Hz, 10-12Hz,13-20 Hz and between 30-130 Hz (*au*, *3-9Hz*, 1.04±0.03 vs. 0.79±0.0, $t_{(8)}$=3.058, p=0.016; *10-12Hz*, 1.08±0.06 vs. 1.3 ±0.13 $t_{(8)}$=-2.43, p=0.041; 13-20Hz, 1.15±0.07 vs. 0.77±0.03 z=-2.666 p=0.008; *30-130 Hz,* 1.07±0.06 vs. 1.4±0.08, z=-2.31 p=0.021). These results indicated that delta, theta, alpha, beta, and gamma bands were significantly different when the baseline vehicle/vehicle ratio was compared with the baseline MK801/MK801 ratio. In this way, all frequencies diminished their power except for the gamma band that was augmented.

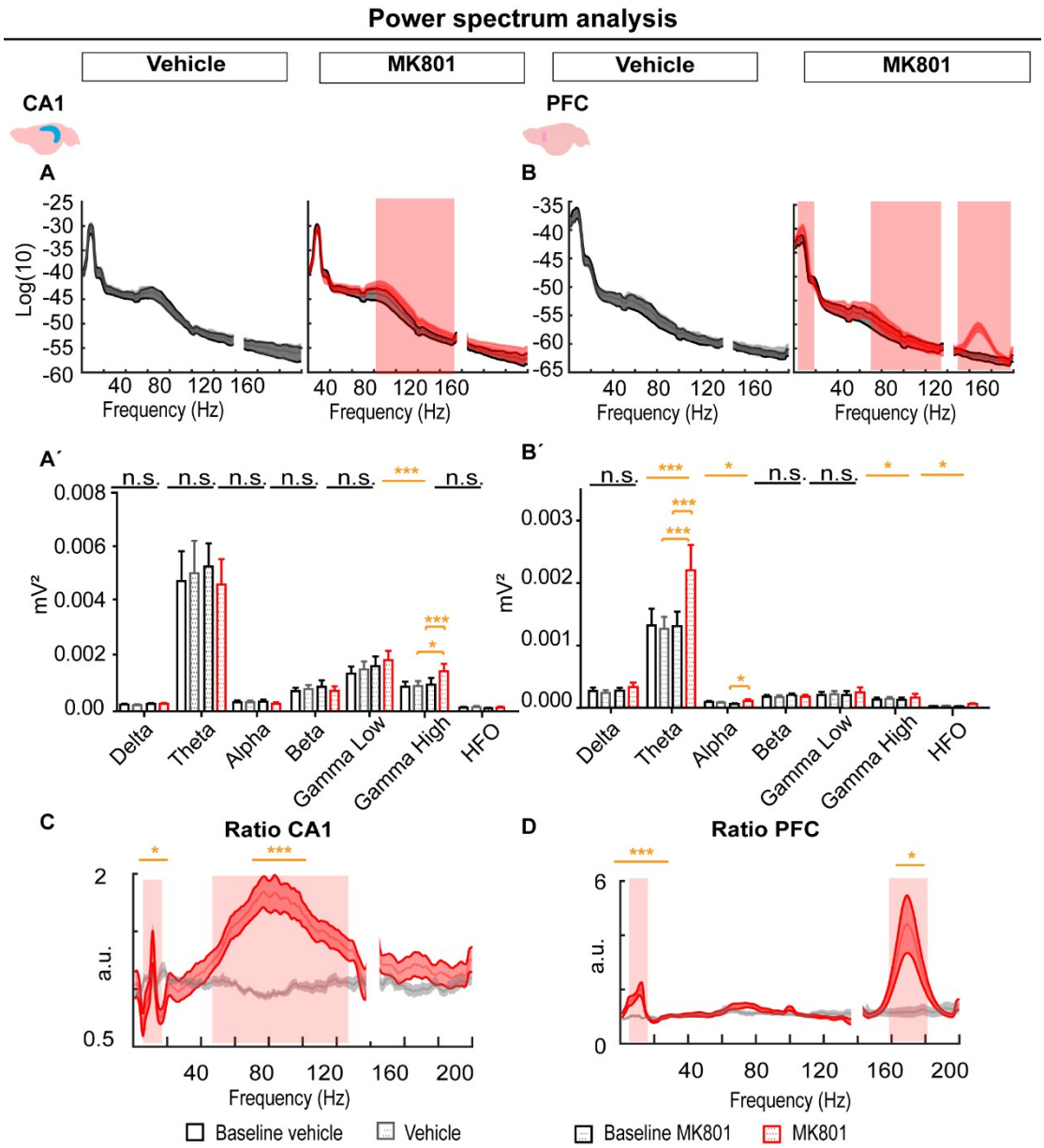

Figure 5. MK801 administration disrupted oscillatory activity in the CA1 and the PFC. A and A' Power spectrum and mean values for each band obtained in the baselines, vehicle and MK801 conditions. Significant differences were found for the high gamma band in the MK801 vs. its baseline and the vehicle condition. B and B'. Prefrontal cortex power spectrum and mean values for each band across the different conditions. Significant differences were observed for theta, alpha, high gamma and HFO. All these differences were explained by changes in the MK801 condition. Note the high increase of theta and HFO. C and D. Ratio of power change obtained between baseline conditions vs. vehicle and MK801. Significant differences were mostly coherent with mean power value analysis. Shadowed regions indicate bands in which significant differences were found.

In the monopolar configuration of the PFC, the comparison between the ratios baseline/vehicle and baseline/MK801 indicated that frequency bands between 0.9 to 16

Hz, including delta, theta and alpha, and HFO were significantly increased in the MK801 condition (*au*, *0.9-16Hz,* 0.99±0.03 vs. 1.5±0.1; $t_{(8)}$=-4.188, p=0.003; *HFO* 1.25±0.2 vs. 2.87±0.5,;$t_{(8)}$=-3.212, p=0.026). We then looked for the ratio of change in the PFC after bipolar derivation finding significant changes between 0.9-16 Hz, 65-100 Hz and in the HFO band (*au*, *0.9-16Hz,* 0.99±0.05 vs. 1.5±0.1; $t_{(8)}$=-2.737, p=0.026; *65-100 Hz* 1.05±0.04 vs. 1.28±0.06; $t_{(8)}$=-3.212, p=0.012; *HFO,* 0.9±0.02 vs. 1.8±0.3, $t_{(8)}$=-2.612, p=0.031). As we observed changes in the theta and HFO in the ratio analysis, we performed pairwise comparison of these oscillatory bands. Further paired comparison in the oscillatory power of these bands found significant increase of power in theta and HFO when the MK801 baseline condition was compared with the MK801 (baseline *vs. MK801, theta, mV^2,* 0.00041±0.0.0001vs. 0.00088±0.0.0004; z=-2.429, p=0.015, Wicoxon ; *baseline vs. the MK801,* HFO *mV^2,* 0.000020±0.000008 0.000032±0. 0.000013; z=-2.192, p=0.028, Wilcoxon).

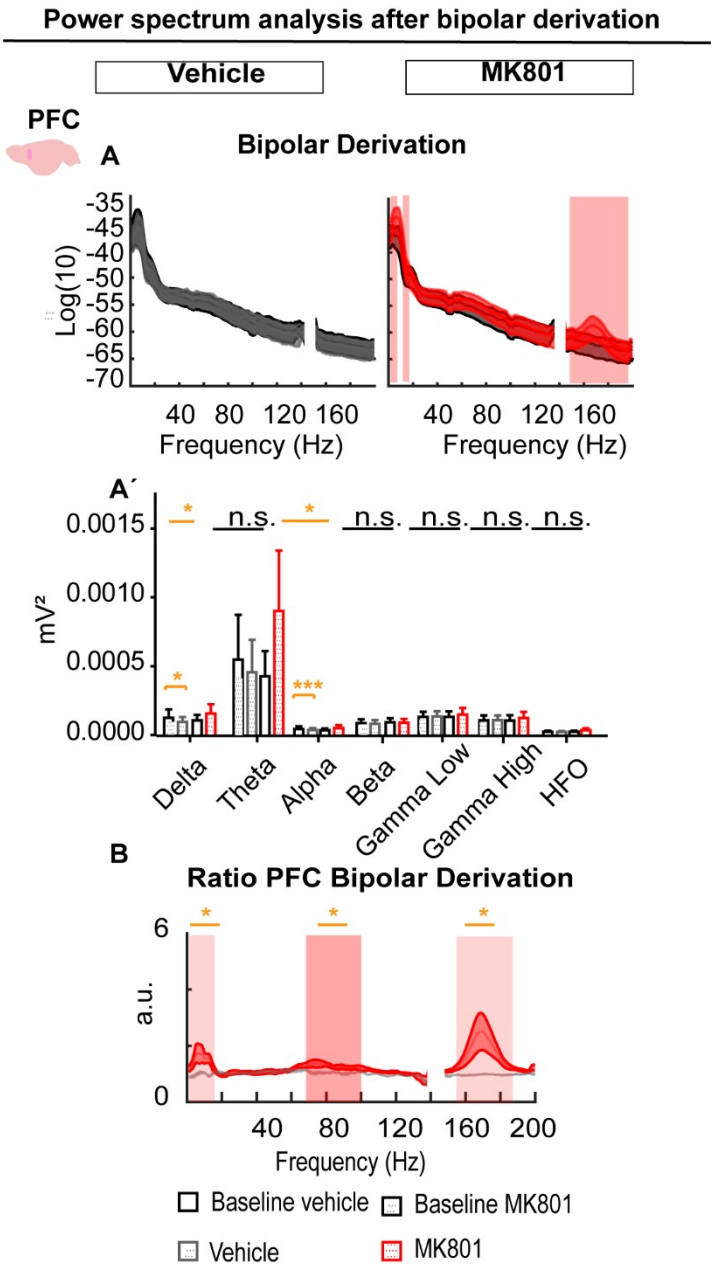

Figure 6. **PFC oscillations analysis after bipolar derivation**. A and A´. Power spectrum and mean power values for the PFC. B. Ratio of change, results were very similar to the monopolar configuration, showing significant changes for low frequencies, including delta, theta and alpha and for HFO. Shadowed regions indicate bands in which significant differences were found

Thus, NMDAr blocking by MK801 affected oscillatory bands in the hippocampus and the prefrontal cortex differently, increasing gamma oscillatory activity in the hippocampal region and in the PFC, where also, theta, alpha, and HFO were augmented.

Effects of MK801 on theta-gamma co-modulation

In the hippocampus, theta-gamma modulation proceeds in an organized manner, with an increase in low gamma power, 30-60 Hz, after the peak of theta (Buzsáki et al., 2003; Valero and de la Prida, 2018). Based on previous work (Korotkova et al., 2010) we calculated a theta/gamma modulation index (GMI). We obtained this index for the analysis of LFPs recorded in the hippocampus and PFC. We obtained the GMI for theta/low gamma 30-65 Hz, theta/high gamma, 66-130 Hz, and for theta/HFO co-modulation in the PFC. Similar to previous work, we performed this analysis in the single-ended configuration (Tamura et al., 2017), see fig 7.

First, to determine the existence of differences due to the treatment condition in the CA1 region, we performed a repeated measure ANOVA for theta/ low gamma and then theta /high gamma modulation, see fig 7C and 7D. We found significant difference for the theta/ low-gamma co-modulation but not for the theta/ high gamma co-modulation (*theta/low gamma,* $f_{(3,24)=}$ 8.469, p=0.001, η^2=0.514,; β=0.983; *theta/high gamma,* $f_{(3,24)=}$ 0.572, p=0.639, η^2=0.067, β=0.15). Then, we explored the differences between each condition for CA1 theta/ low-gamma co-modulation. We found that the theta/gamma co-modulation increased in a no significant manner during the vehicle condition (baseline vs. vehicle, 0.20±0.02 vs. 0.23±0.02; $t_{(8)}$= -2.307, p=0.05). On the other hand, MK801 significantly reduced theta/gamma co-modulation during the exploration in the open field (baseline MK801 vs. MK801, 0.18±0.01 vs. 0.12±0.01; $t_{(8)}$=3.974, p=0.004). No significant differences were found between *baseline vehicle vs. baseline MK801*, ($t_{(8)}$=0.977, p=0.357). However, we found significant differences between the vehicle vs. the MK801 ($t_{(8)=}$4.097, p=0.003). Significant changes were preserved after Bonferroni corrections, (p=0.0125).

Then we investigated theta/gamma co-modulation of the LFP recorded in the PFC finding significant difference for theta-low gamma co-modulation and theta-high gamma co-modulation ($f_{(2,15)=}$ 14.364, p=0.0000, η^2=0.642, β=0.993; $f_{(3,24)=}$ 39.961, p<0.000, η^2=0.833, β=1), see fig 7E and 7F. Then, we aimed to determine possible statistical difference between specific conditions. We observed no significant changes between the baseline and vehicle, but a significant decrease in theta/ low gamma modulation after MK801 administration (a.u., *baseline vs. vehicle,* 0.09±0.01 vs. 0.11±0.01; $t_{(8)}$=-1.814, p=0.107, *baseline MK801 vs. MK801,* 0.12±0.004 vs. 0.05±0.009; $t_{(8)}$= 4.897, p=0.001). No significant differences were observed between the baseline vehicle vs. the baseline MK801 ($t_{(8)}$=1.713, p=0.125). We detected significant differences when we compared the vehicle vs. the MK801 condition ($t_{(8)}$= 4.69, p=0.002). Significant results

were preserved after Bonferroni corrections ($p<0.0125$). When we investigated the theta/high gamma band co-modulation, we found a higher index in the vehicle condition vs. baseline, and a significant decrease after MK801 administration (*baseline vs. vehicle,* 0.09±0.004 vs. 0.11±0.007; $t_{(8)}= -3.706$, $p=0.006$; *baseline vs. MK801* 0.08±0.004 vs. 0.04 ±0.003; $t_{(8)}= 8.144$, $p=0.000$). We observed no significant changes between the two baseline conditions ($t_{(8)}= 1.739$, $p=0.12$). Then, we observed that values for the MK801 recordings were significantly lower than in the vehicle condition ($t_{(8)}= 10.52$, $p=0.0000$). Significant results were preserved after Bonferroni corrections ($p<0.0125$). The emergence of HFO in the PFC was strongly linked with theta oscillatory activity, therefore we investigated if this co-modulation was significantly different due to drug treatment. We found significant differences across conditions ($f_{(2,15)=}$ 25.549 $p=0.0000$, $\eta^2=0.762$; $\beta=1$). Observed changes were explained by the administration of MK801 (*baseline vs. vehicle,* 0.08±0.01 vs. 0.8±0.01; $t_{(8)}= -0.325$, $p=0.753$; *baseline vs. MK801,* 0.06±0.007 vs. 0.29±0.03; $t_{(8)}= -5.071$, $p=0.0001$; vehicle vs. MK801; $t_{(8)}= -4.825$, $p=0.001$), see Fig 7H and 7I. Significant results were preserved after Bonferroni corrections ($p<0.0125$).

These data suggest that NMDAr blocking by MK801 impaired theta-gamma co-modulation in the hippocampus, and generated HFO linked to local theta oscillations co-modulation in the PFC during spontaneous exploration.

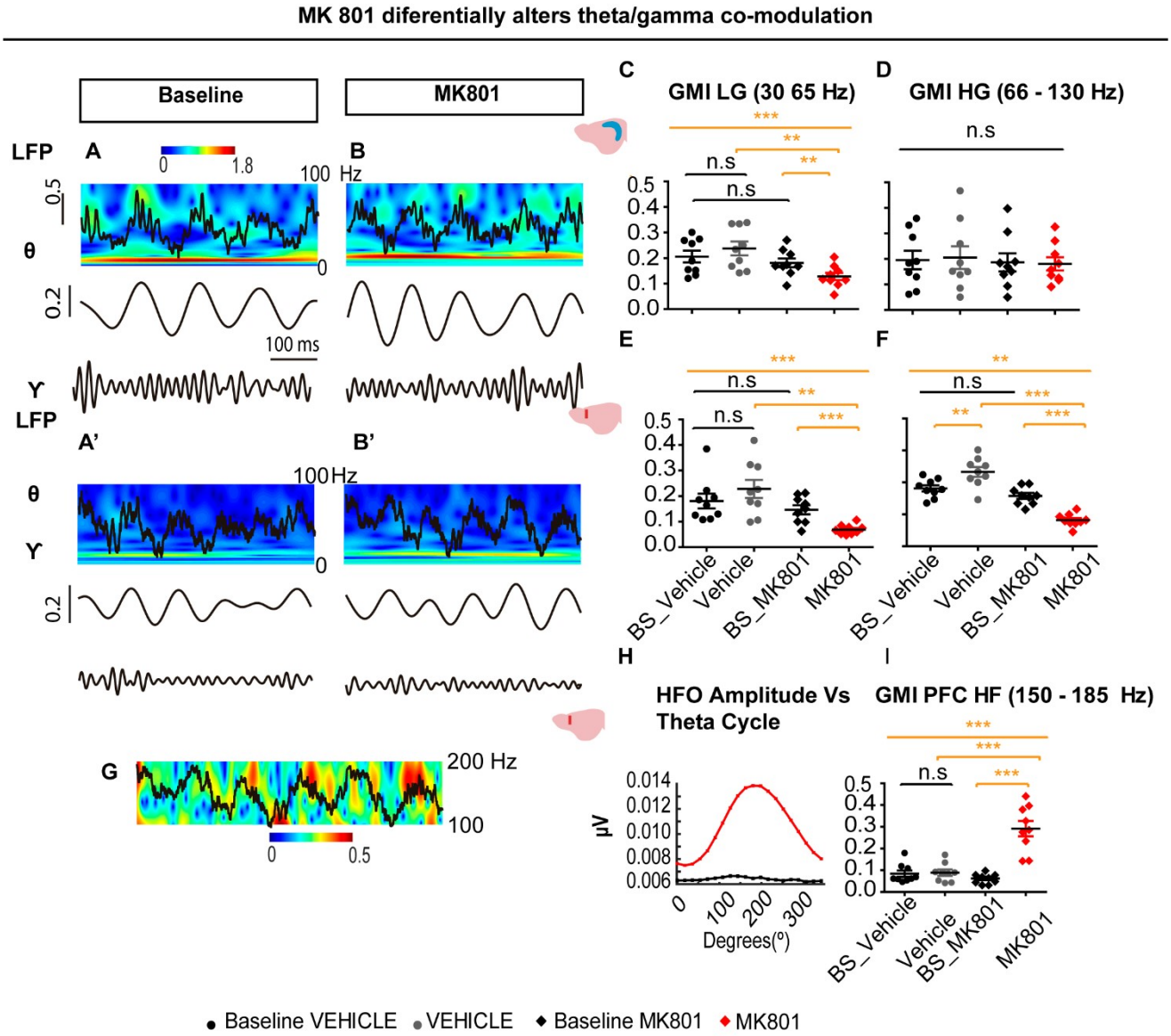

Figure 7. MK801 administration disrupted theta/gamma co-modulation. A Representative local field potential, wavelet, and filtered signal for theta and gamma in CA1 during the baseline. A´ Similar representative results in PFC, same condition. B. Representative recordings obtained in CA1 after MK801 administration. B.´ Representative recordings in the PFC and after MK801 administration. Note the higher amplitude in PFC of theta oscillations during the MK801 condition. C. Theta/gamma co-modulación in the CA1 region showed significant differences due to MK801 administration. D. CA1 Theta/high gamma was not significantly modified by MK801. E. PFC Theta/low gamma was significantly reduced after MK801 administration. F. Similar results were found for theta/ high gamma co-modulation. G. Raw LFP recorded in PFC. Wavelet analysis revealed the strong modulation of HFO after NMDAr blockade. H. HFO amplitude was modulated by the theta phase I. Theta/HFO significantly increased by MK801.

Effects of MK801 on hippocampal-PFC interaction during spontaneous exploration.

As a measure of brain area coordination, we investigated the coherence for each frequency band in a single-ended electrode configuration. To determine the existence of differences due to the treatment condition we performed repeated measure ANOVA and Friedman no parametric test. We observed no significant changes in the baseline vs. the vehicle condition for any of the frequency bands (*delta*, $f_{(3,24)=}$ 0.848 p=0.481, η^2=0.096, β=0.2; *theta*, $f_{(3,24)=}$ 1.633, p=0.208, η^2=0.170, β=0.37; *alpha*, $f_{(2,12)=}$ 0.423, p=0.614, η^2=0.05, β=0.1; *beta,* $\chi^2_{(3)=}$ 3.0 p=0.3924; *low gamma,* $\chi^2_{(3)=}$ 4.467, p=0.215; *High gamma,* $\chi^2_{(3)}$ =3.533, p=0.316; *HFO*, $\chi^2_{(3)=}$ 3.533 p=0.316). To control for possible signal volume propagated from other regions, we calculated the same coherence values after applying a bipolar derivation. These results did not differed from those obtained in the monopolar configuration (*delta*, $f_{(3,24)=}$ 1.633, p=0.208, η^2=0.17; β=0.373; *theta*, $f_{(3,24)=}$ 1.633, p=0.208, η^2=0.170, β=0.37; *alpha*, $f_{(2,12)=}$ 1.859, p=0.164; η^2=0.0.18, β=0.42; *beta,* $X^2_{=}$ 3.0, p=0.3924; *low gamma,* X^2= 4.467, p=0.215; *High gamma,* $\chi^2_{(3)=}$ 3.153, p=0.316; *HFO*, $\chi^2_{(3)=}$ 3 , p=0.392).

Visual comparison of the distribution indicated the existence of possible differences between the MK801 and its baseline for the delta band in the monopolar and bipolar configuration. Therefore, we performed paired comparisons finding a minimal but significant increase for the delta band in the monopolar and bipolar configuration (monopolar, *delta, r,* 0.60±0.005 vs. 0.63±0.01; $t_{(8)}$= -2.54, p=0.0340; *bipolar,* 0.55±0.006 vs. 0.57±0.005, $t_{(8)}$= -3.01, p=0.009) . Similarly, we observed a significant coherence augmentation for the alpha band in the bipolar configuration (*alpha*, *r*, 0.55±0.006 vs. 0.57±0.005, $t_{(8)}$= -3.01, p=0.016).

Long-range co-modulation of theta/gamma activity has been proven relevant for the interaction of the hippocampal and PFC (Tamura et al., 2017). Thus, we wanted to determine if the interaction between CA1 theta and PFC gamma was altered after NMDAr blockade. We calculated the GMI between the ongoing theta in CA1 and the gamma band recorded in the PFC, and we determined the existence of differences due to the treatment condition. We found significant difference for the theta/ low gamma and high gamma co-modulation (theta/low gamma, $f_{(2,12)=}$ 21.423 p=0.000, η^2=0.728, β=0.9theta/high gamma $X_{(3)}^2$*=22.6, p=0.000*) , and also for the theta/ HFO (X^2*=8.733,*

p=0.033). Then we compared specific conditions and we found that theta/gamma modulation was increased in the baseline vs. vehicle condition for low, high gamma and HFO (*low gamma,* 0.08±0.012 vs. 0.11±0.015; $t_{(8)}$= -3.30, p=0.011; *high gamma*, 0.051±0.008 vs. 0.08±0.01; Z=-2.666, p=0.008 ; *HFO,* 0.04±0.008 vs. 0.006±0.008; Z=-2.31, p=0.021). Then, we compared the MK801 baseline vs. the MK801 condition. We observed that the theta/gamma modulation index was significantly reduced for low and high gamma. However, we found no significant changes for HFO (*low gamma,* 0.09±0.006 vs. 0.04±0.004; $t_{(8)}$= 10.344, p=0.000; *high gamma*, 0.06±0.007 vs. 0.04 ±0.002; $t_{(8)}$= 2.921, p=0.019; *HFO,* 0.042±0.004 vs. 0.08±0.016; $t_{(8)}$= -2.172, p=0.062). When we compared the vehicle with the MK801 we observed significant difference for the theta/ low and high gamma but not for the theta/HFO (*low gamma* $t_{(8)}$= 5.749, p=0.000; *high gamma*; $t_{(8)}$= 3.250, p=0.0012; *HFO* $t_{(8)}$= -2.172, p=0.062), see fig 8.

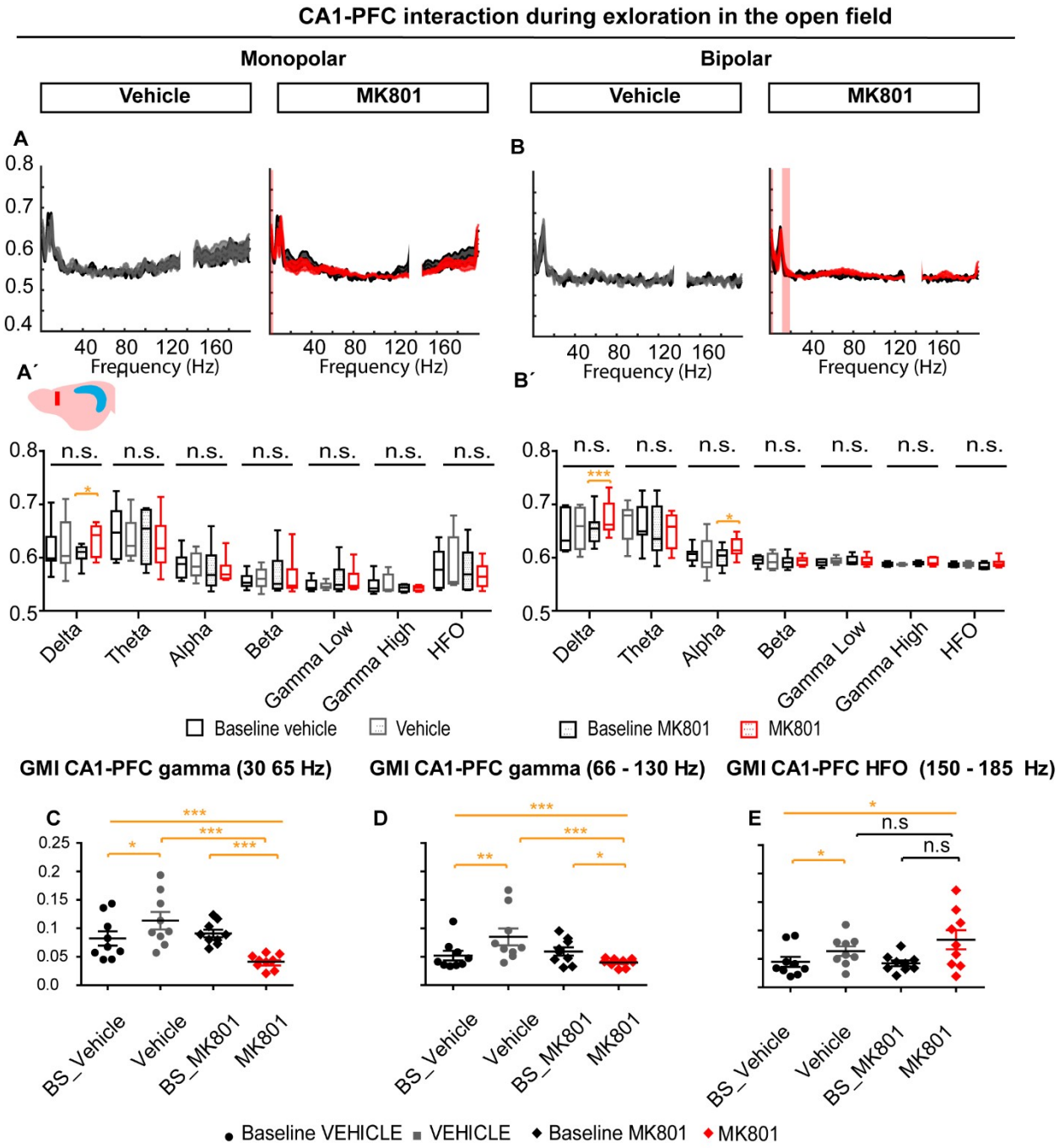

Figure 8. MK801 administration altered CA1-PFC interaction changing theta/gamma co-modulation. A. Coherence values for the baseline vs. vehicle and baseline vs. MK081 obtained in single electrode configuration. A'. Mean coherence values by oscillatory band. B. Coherence values for the bipolar configuration. B' Mean coherence distribution for different bands. C. Long range theta/low gamma co-modulation. Significant differences are described by each comparison of interest. D. Theta/high gamma co-modulation. E. Theta/HFO co-modulation.

Hippocampal oscillatory activity during correct and incorrect trials.

We classified correct vs. incorrect alternations and then we analyzed the power spectrum, coherence, and theta/gamma modulation in the CA1 and PFC. To control for the locomotor activity accompanying correct and incorrect alternations, we investigated if there were differences in the speed of movement in the different trial types, correct vs. incorrect and between experimental conditions. First, we could verified the existence of significant differences ($f_{(3,18)=}$ 26.851 p=0.000; η^2=0.871; β=1). Further analysis demonstrated that differences were due to drug condition but not to trial type (*baseline correct vs. incorrect, speed:* 0.12±0.007 vs. 0.10±0.009, $t_{(8)}$= 1.31, p=0.260; *MK801 correct vs. incorrect*: 0.18± 0.01 vs. 0.17± 0.013, $t_{(6)}$=1.9, p=0.12; *correct baseline vs. correct MK801*, $t_{(8)}$= -7.08, p=0.000; *incorrect baseline vs. incorrect*, $t_{(6)}$=-5.158, p=0.002), see Fig 9A. These results support the idea that possible differences in oscillatory activity during trial type are not related to basic motor behavior but might be due to cognitive processes.

Therefore, we looked at the different oscillatory bands linked to spatial navigation and working memory. We observed no significant differences for CA1 theta power spectrum when compared between trial type and treatment conditions, ($f_{(3,18)}$=1.259, p=0.318, η^2=0.173, β=0.279). We observed a significant difference for the low gamma (X^2=9.343, p=0.025). This significant difference was explained by the drug condition but not by trial type (*baseline correct vs. incorrect,(mV^2),* 0.0016±0.000 vs. 0.0015±0.000; *z*=-0.169, p=0.866; *MK801 correct vs. incorrect,(mV^2),* 0.0019±0.000 vs. 0.18±0.000; *z*=-1.183, p=0.237; *baseline correct vs. MK801 correct; z*=-2.366, p=0.018; *baseline incorrect vs. MK801 incorrect; z*=-2.028, p=0.043, *Wilcoxon*), however this difference was not significant after Bonferroni corrections for the adjusted levels of significance (p=0.0125). Then, we investigated gamma activity finding significant difference for high gamma ($\chi^2_{(3)}$=17.914, p=0.000, *Friedman*). This difference was explained by drug treatment but not by trial type (*baseline correct vs. incorrect, (mV^2),* 0.0011±0.000 vs. 0.009±0.000; *z*=-0.169, p=0.866; *MK801 correct vs. incorrect,* 0.0017±0.000 vs. 0.0016±0.000; $t_{(6)}$=*2.142*, p=0.076; *baseline correct vs. MK801 correct,*, *z*=-2.366, p=0.018; *baseline incorrect vs. MK801 incorrect,* $t_{(6)}$=*-7.186*, p=0.000).

Then, to determine if CA1 theta/gamma modulation was relevant for memory performance, we obtained the GMI for low gamma in the CA1 region and we compared them between trial type and drug, see fig 9B and 9C. We found significant differences for the theta/low gamma co-modulation ($f_{(3,18)}$=11.889, p=0.000, η^2=0.665,β=0.094).

Again, significant difference was explained by the drug condition but not by trial type (*baseline correct vs. incorrect, (a.u.)* 0.33±0.02 vs. 0.3±0.03; $t_{(6)}$=1.110, p=0.310; *MK801 correct vs. incorrect.* 0.23±0.01 vs. 0.21±0.01; $t_{(6)}$=1.567, p=0.168; *baseline correct vs. MK801 correct;* $t_{(6)}$=4.162, p=0.006; *baseline incorrect vs. MK801 incorrect,* $t_{(6)}$=4.404, p=0.007). Then we explored the theta/high gamma co-modulation. We observed the existence of significant differences ($f_{(3,18)}$=11.52, p=0.015; η^2=0.658; β=0.8). Paired t-test demonstrated an effect based on trial type for the baseline condition (*baseline correct vs. incorrect, (a.u.)* 0.26±0.03 vs. 0.29±0.03, $t_{(6)}$=-2.639, p=0.039) but not for the MK801 condition (*MK801 correct vs. incorrect.* 0.25±0.02 vs. 0.23±0.03, $t_{(6)}$=2.021, p=0.09). No significant differences were found for the GMI for correct trials across conditions (baseline *correct vs. MK801 correct,* $t_{(6)}$=0.534, p=0.612), but there were significant difference for the incorrect trials (*baseline incorrect vs. MK801 incorrect,* $t_{(6)}$=5.583, p=0.001).

PFC oscillatory activity during correct and incorrect trials

Then, we investigated the oscillatory activity obtained from the PFC recordings. First, our analysis verified that there was no significant difference in the theta band ($f_{(3,18)}$=3.145, p=0.087; η^2=0.344; β=0.4). With respect to gamma bands we observed a significant change for the low gamma across the different conditions ($X_{(3)}^2$=10.714, p=0.013). This was explained by the drug condition but not by trial type (*baseline correct vs. incorrect,(mV²)* 0.0002±0.000 vs. 0.00019±0.000, *z*=-0.845, p=0.398; *MK801 correct vs. incorrect, ,(mV²)* 0.0002±0.000 vs. 0.00019±0.000 *z*=-0.507, p=0.612; *baseline correct vs. MK801 correct, z*=-1.859, p=0.063; *baseline incorrect vs. MK801 incorrect, z*=-2.366, p=0.018, Wilcoxon) , therefore, no specific pattern associated with correct or incorrect trial type was observed, also this difference was not significant after Bonferroni corrections (p=0.0125). Regarding the high gamma band, e observed no significant difference $f_{(3,18)}$=3.372, p=0.11; η^2=0.36; β=0.358).

To investigate if PFC theta/gamma modulation was relevant for memory performance, we obtained the GMI for low and high gamma in the PFC. We explored if there were significant differences due to trial type and drug condition, see fig 9D and 9E. We found significant differences for the theta/low gamma co-modulation ($f_{(3,18)}$=5.232, p=0.009; η^2=0.466, β=0.859). This difference was not due to correct vs. incorrect trial type in the baseline and the MK801 condition (*baseline correct vs. incorrect, (a.u.)* 0.26±0.04 vs. 0.23±0.02; $t_{(6)}$=1.229, p=0.265; *MK801 correct vs. incorrect.* 0.17±0.01 vs. 0.16±0.03; $t_{(6)}$=0.351, p=0.738). Then, we explored possible difference due to drug treatment finding significant difference only for the baseline incorrect vs. MK801 incorrect trials

(baseline *correct vs. MK801 correct,* $t_{(6)}$=2.145, p=0.076; *baseline incorrect vs. MK801 incorrect,* $t_{(6)}$=2.536, p=0.04). This difference was not significant after Bonferroni corrections. Then we investigated the theta/high gamma co-modulation finding significant differences ($f_{(3,18)}$=7.659, p=0.002; η^2=0.561, β=0.963). Paired t-test demonstrated an effect based on trial type for the baseline condition (*baseline correct vs. incorrect, (a.u.)* 0.16±0.01 vs. 0.19±0.01; $t_{(6)}$=-4.385, p=0.005) and for the MK801 condition (*MK801 correct vs. incorrect.* 0.16±0.01 vs. 0.10±0.01; $t_{(6)}$=2.73, p=0.034). No significant differences were found for the correct trials across drug conditions (baseline *correct vs. MK801 correct,* $t_{(6)}$=-0.097, p=0.926), but there was a significant difference for the incorrect trials (*baseline incorrect vs. MK801 incorrect,* $t_{(6)}$=4.463, p=0.004). Differences were preserved after Bonferroni corrections (p=0.0125).

CA1-PFC interaction during y-maze

Once we analyzed the oscillatory activity in CA1 and the PFC, we looked to the communication between the hippocampus and the PFC, see fig 9F and 9G. First we looked for changes in theta coherence across trial type, correct and incorrect, and a possible difference pattern across drug conditions, finding no significant differences ($f_{(3,18)}$=1.047, p=0.396, η^2=0.149, β=0.237). Similarly, we found no significant difference for low and high gamma coherence ($X_{(3)}^2$=0.429, p=0.934; $X_{(3)}^2$=5.057, p=0.168). We then explored the long-range hippocampal theta and PFC gamma co-modulation. We found significant differences for the low gamma ($f_{(3,18)}$=8.858, p=0.001, η^2=0.596; β=0.982). This significant difference was explained by drug treatment but no pattern was observed for trial type (*baseline correct vs. incorrect, (a.u.)* 0.26±0.02 vs. 0.25±0.03; $t_{(6)}$=0.122, p=0.907; *MK801 correct vs. incorrect.* 0.19±0.01 vs. 0.14±0.01; $t_{(6)}$=2.403, p=0.053; baseline *correct vs. MK801 correct,* $t_{(6)}$=2.055, p=0.086; *baseline incorrect vs. MK801 incorrect,* $t_{(6)}$=3.866, p=0.0048). On the other hand no significant difference was found for the high gamma ($f_{(3,18)}$=2.630, p=0.082, η^2=0.305, β=0.545).

CA1-PFC theta/gamma co-modulation correlated with the performance in the y-maze.

As we found a trial type relation with theta/gamma co-modulation we explored if the theta/gamma co-modulation obtained for the complete y-maze recording session correlated with the performance of mice in the baseline and in the MK801 condition (see Fig 10). First, we investigated the possible relationship between the theta/gamma co-modulation in the baseline. We observed that the CA1 theta/ low gamma and high gamma did not correlate in a significant manner with performance (CA*1 theta/low*

gamma, r=0.261, p=0.572; *theta/high gamma,* r=-0.0*39*, p=0.935). Then we looked at theta/gamma co-modulation in the PFC. We found that both theta/gamma co-modulation values presented higher correlations with the performance of mice however these were not significant (*PFC theta/low gamma,* r=0.673, p=0.098; *theta/high gamma,* r=0.467, p=0.29). Long-range co-modulation between CA1 and PFC was also investigated. We observed that CA1-PFC theta/low gamma co-modulation significantly correlated with the performance while the high gamma presented a positive but not significant correlation (*CA1PFC theta/low gamma,* r=0.88, p=0.009; *theta/high gamma,* r=0.563, p=0.188). Then, we investigated the effects of NMDAr blockade in the relationship between theta/gamma co-modulation and performance finding no significant correlations (*CA1 theta/low gamma,* r=0.142, p=0.76205; *CA1 theta/high gamma,* r=-0.195, p=0.675; *PFC theta/low gamma,* r=0.408, p=0.364; *PFC theta/high gamma,* r=-0.265, p=0.566; *CA1PFC theta/low gamma,* r=0.239, p=0.605; *theta/high gamma,* r=0.358 p=0.431). We could verify further that the correlation for CA1-PFC theta/low gamma vs. performance was significantly lower after MK801 administration ($t_{(6)}$=3.291, p=0.017).

These results indicated that long-range theta/gamma co-modulation might be relevant for memory performance in the y-maze and that MK801 administration disrupts the communication between the CA1 and the PFC.

We investigated this further exploring possible relation between the power spectrum and coherence values during the complete y-maze session and the animal's performance. No significant correlation was found for any of the frequency bands, neither in power nor coherence, (data not shown).

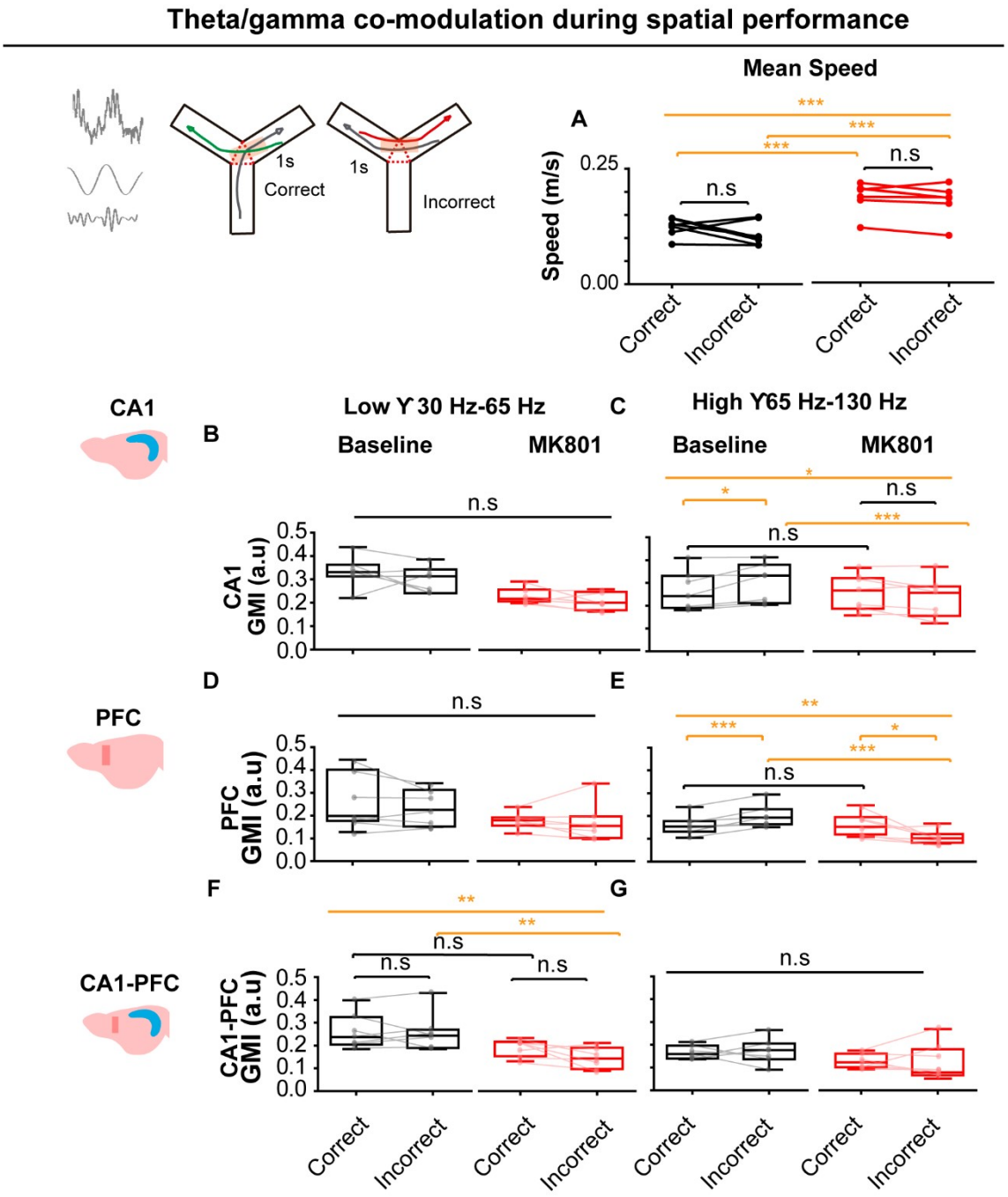

Figure 9. Theta/high gamma co-modulation in CA1 and the PFC was significantly different between correct and incorrect trials. Dots indicate individual animals. Lines connect values from the same animal across correct and incorrect trials. A. Significance difference in the speed of movement was due to drug treatment but not to trial type, correct vs. incorrect. B and D No significant differences were found for theta/low gamma co-modulation in the CA1, and the PFC. C and E. Theta/high gamma co-modulation was significantly different between correct and incorrect trials in the CA1 and the PFC, revealing an oscillatory pattern for correct vs. incorrect trials. While the GMI was higher in the incorrect trials in the baseline, this changed after MK801 administration. In the MK801 condition, correct

trials showed similar values to correct trials of the baseline condition, however the co-modulation in the incorrect trials was higher. F. CA1-PFC Theta/ low gamma co-modulation was significantly lower when incorrect trials baseline vs. MK801 were compared. G. No significant changes were found for the theta/high gamma co-modulation.

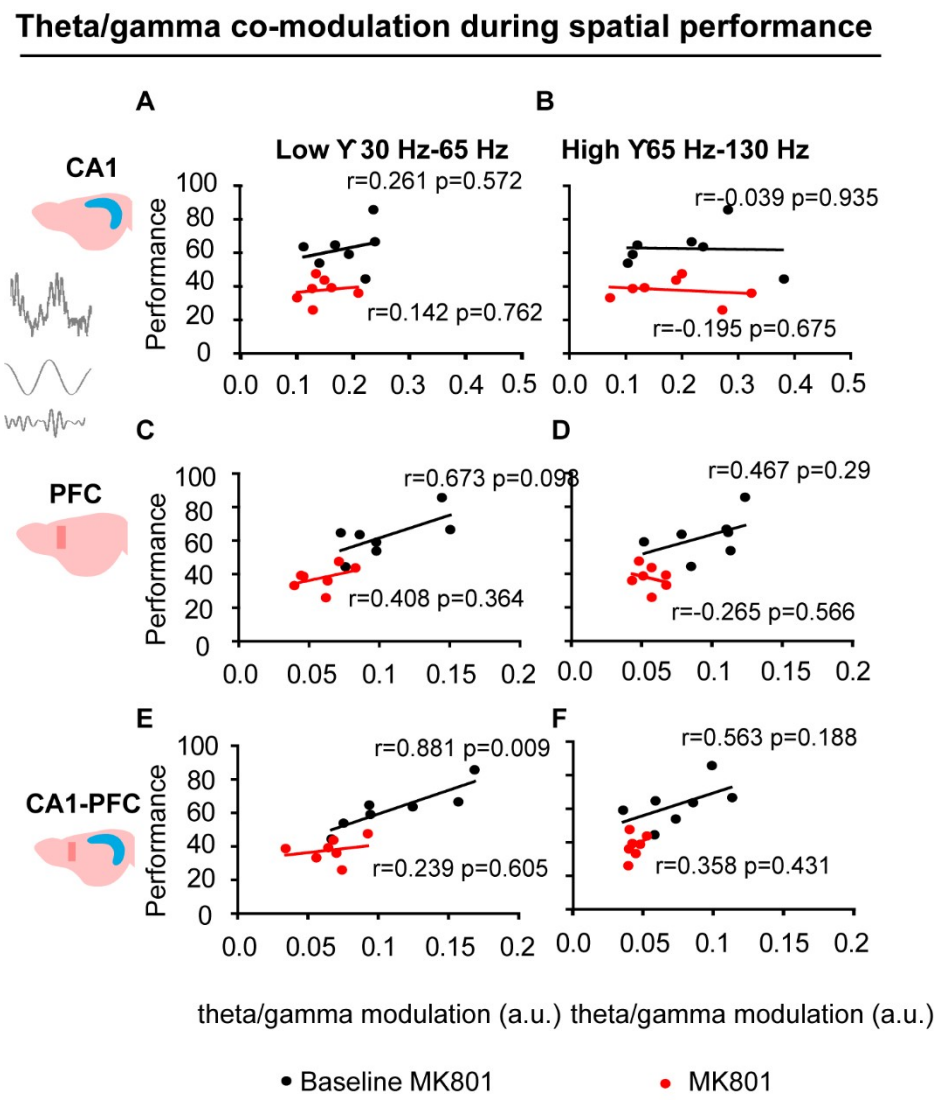

Figure 10. Theta/gamma co-modulation and performance in the y-maze. A, and B. CA1 Theta/ low and high gamma did not significantly correlate with performance in the y-maze. C and D. Similarly, PFC theta/gamma co-modulation did not correlate with y-maze performance. E. Hippocampal-PFC long-range theta/low gamma correlation was significantly correlated with the performance in the y-maze. This correlation was disrupted by MK801 administration. F. Hippocampal-PFC Theta/high gamma was not significantly correlated with the performance.

Discussion

NMDAr blockade induced positive-like and cognitive symptoms.

Positive symptoms such as hallucinations, delusions, or hyperactivity are one of the hallmarks of SCZ and psychotic episodes (Owen et al., 2016). Throughout our experiments, MK801 induced hyperlocomotion, increasing the speed of movement, exploratory time, and the total number of entries in the y-maze. The augmentation of motor behavior was consistent in the open field and the y-maze and could be interpreted as reproducing SCZ's positive symptoms. As previously described, this hyperactivity correlates with increased levels of dopamine release in the striatum, possibly mediated by MK801's action on NMDAr in PV+ interneurons (Belforte et al., 2010; Carlén et al., 2012; Bygrave et al., 2016). On the other hand, animal behavior was very consistent across baseline conditions across different days. Another of the hallmarks of SCZ is its associated cognitive deficits, especially those related to executive function, which are accompanied by aberrant oscillatory activity (Uhlhaas and Singer, 2010; Lewis et al., 2012). In agreement with previous work (Bygrave et al., 2016), NMDAr blockade impaired spatial working memory, a form of executive function, in the y-maze memory test (Callicott et al., 2000; Miedel et al., 2017). This memory deficit was associated with a significant decrease of the long-range theta/gamma co-modulation, indicating a distorted dialog between the hippocampus and the PFC.

Therefore, NMDAr hypofunction might be at the heart of different positive and cognitive symptoms observed in SCZ either directly or indirectly, e.g., mediating the activity of dopamine levels and altering the dialog between different brain regions.

NMDAr blockade altered the relationship between hippocampal oscillations and locomotion.

In physiological conditions, different aspects of theta and gamma oscillations correlate with the speed and the acceleration of movement, mediating spatial cognition (Whishaw and Vanderwolf, 1973; Chen et al., 2011; Long et al., 2014; Kropff et al., 2021). This is further supported by the fact that the association strength between theta and speed predicts the performance in spatial tasks (Richard et al., 2013.; Young et al., 2020). We observed that MK801 disturbed the normal association between speed of movement and oscillations, especially high gamma activity and marginally theta oscillations.

By disrupting the relationship between oscillatory activity and motor behavior, NMDAr hypofunction might cause the loss of spatial information in place cells, the impairment of the internal odometer and therefore the integration of egocentric and allocentric information. Also, oscillatory changes could generate the functional disconnection between different brain regions (Jackson et al., 2004; Terrazas et al., 2005; Inostroza et al., 2013; AA, Housh et al, 2014).

NMDAr blockade differentially altered the oscillatory activity in the hippocampus and PFC.

Previous work indicated that NMDAr blockade produced similar effects across different brain regions. However, in our experiments MK801 produced different oscillatory profiles in the hippocampus and PFC. While oscillatory changes in the CA1 were characterized by changes in the gamma power, oscillatory activity under MK801 in the PFC was characterized by an increase in theta, beta, high gamma and HFO. Unlike in previous reports (Olszewski et al., 2013), changes in the PFC oscillations, including theta, gamma, HFO, etc., were maintained after bipolar derivation, as revealed by the analysis of ratios, (baselines/experimental condition). Reductions of hippocampal theta have been described in previous work (Hargreaves et al., 1997; Kittelberger et al., 2012; Kiss et al., 2013) and to our knowledge, there is no previous evidence of theta power augmentation after NMDAr blockade. The differential effect in hippocampal theta vs. PFC theta, indicates that the increase of theta power in the PFC region is not propagated, at least by the activity generated by the hippocampus.

The emergence of HFO in the PFC following NMDAr blockade is an intriguing phenomenon. We hypothesized that this increase is possibly produced by the alteration of the firing frequency of interneurons and pyramidal neurons and/or the desynchronization of different clusters of neurons (Homayoun and Moghaddam, 2007; Ibarz et al., 2010). On the other hand, the strong relationship between theta activity and high HFO oscillations suggests that this is organized by the local theta. This is a very interesting phenomenon that needs further attention.

Our results indicate that MK801 produced small changes in the dialog between the hippocampus and PFC as indicated by the frequency coherence analysis. However, paired comparisons, showed that MK801 increased the coherence in the delta band also augmenting the coherence in the alpha band in the monopolar configuration analysis. Therefore, changes in the dialog between the hippocampus and the PFC did not affect theta oscillations, associated with spatial working memory. However, the

theta/gamma modulation between the hippocampus and PFC was significantly diminished after MK801 administration, indicating a role of NMDAr in the interaction and coupling of different bands across distantly located circuit nodes. As previously mentioned, it is relevant to highlight that HFOs recorded in the PFC were not modulated by hippocampal theta after NMDAr blockade, further supporting the idea that HFOs in the PFC are locally generated and independent from hippocampal activity. The alteration of long-range modulation and the local disruption of theta/gamma activity might be caused by shared physiological mechanisms in different structures.

The circuits connecting the hippocampus and the PFC are complex. The PFC receives direct inputs from the intermediate, ventral hippocampus, the subiculum, and indirect inputs from the dorsal hippocampus through the thalamic nucleus. Therefore, the different components of the circuit might mediate different aspects of information processing. Hence, future work should aim to record from the dorsal and ventral hippocampus and subiculum, relevant thalamic nuclei as well as the PFC simultaneously (Hoover et al., 2007; Adhikari et al., 2009; Sigurdsson and Duvarci, 2016; Tamura et al., 2017).

NMDAr blockade diminished theta/gamma co-modulation.

The co-modulation of different frequency oscillations, especially theta/gamma, is key for the successful organization of neuronal ensemble activity and information processing in local and long-range networks (Sigurdsson et al., 2010; Buzsáki and Watson, 2012; Lopez-Pigozzi et al., 2016; Navas-Olive et al., 2020). MK801 administration reduced theta/gamma co-modulation in the CA1 and PFC. This decrease affected low and high gamma bands, suggesting that theta/gamma coordination depends on NMDAr normal function and most probably on PV+ interneurons (Korotkova et al., 2010; Lopez-Pigozzi et al., 2016). The observed changes in theta and gamma co-modulation activity might be associated with modifications in neuron functioning including changes in the firing rate, spike train organization, and network/neuron loss of coherence (Homayoun & Moghaddam, 2007).

Correct and incorrect trials were specifically associated with theta/gamma co-modulation levels in the hippocampus and the PFC.

Previous work indicates the dialog between hippocampus and the PFC, is necessary for spatial working memory (Sigurdsson et al., 2010; Tamura et al., 2017). We found no specific changes in the power and coherence of different oscillatory bands, linked to

correct and incorrect trials, neither in the baseline or MK801 condition. However, we observed a specific correct vs. incorrect trial pattern associated to the theta/gamma modulation in the hippocampus and the PFC. Thus, hippocampal theta/high gamma co-modulation was significantly lower in the correct vs. the incorrect trials during the baseline condition. However, during the MK801 condition, hippocampal theta/high gamma co-modulation was significantly lower in the incorrect trials. This same trend was found in the theta/ high gamma co-modulation index obtained in the PFC. This might indicate that cross frequency coupling needs to be set at a specific range for information to be properly coded. This idea is further supported by the fact that no significant differences were found between the theta/ high gamma co-modulation for the baseline correct trials vs. the MK801 correct trials. These results are similar to previous work in which theta/gamma co-modulation range was critical for spatial working memory performance (Tamura et al., 2017). In addition, CA1-PFC theta/gamma co-modulation showed no specific pattern due to trial type. This was surprising since theta/gamma low co-modulation obtained during the entire y-maze session was positively correlated with the performance in the y-maze. This relationship was totally disrupted after MK801 administration. Therefore, theta/gamma modulation might be necessary for spatial working memory, helping to coordinate local and long-range networks.

Different factors mediate the effects of NMDAr hypofunction.

Our study found that MK801 alters the typical relationship between oscillations and motor behavior, theta/gamma co-modulation, and cognition. However, the cellular mechanisms underlying these changes need further investigation. It is likely that different cell types bear different roles in NMDAr hypofunction's pathophysiology. This is supported by different work showing that the expression of NMDAr on pyramidal neurons is necessary for MK801's disruption of hippocampus and PFC interaction while NMDAr expression in interneurons appears to mediate the motor effects of MK801 (Belforte et al., 2010; Carlén et al., 2012; Bygrave et al., 2016; Hudson et al., 2020). Previous work demonstrated different interneuron types differentially affects oscillatory activity and cognitive function. Thus, PV+ interneurons partial disconnection of the excitatory-inhibitory circuits specifically affected gamma rhythms and executive function, generating a SCZ-like phenotype. On the other hand, a partial disconnection of cholecystokinin (CCK+) interneurons specifically affected theta oscillations, place cell firing and spatial cognition (delPino et al., 2013; Del Pino et al., 2017). Similarly, we

can expect a different function of NMDAr in different interneuron types. Scrutinizing these possible differences by means of opto-tagging and manipulating NMDAr activity during different conditions would help to unveil the role of NMDAr in micro and macro circuits involved in oscillatory activity, cognition, and the link between both (Royer et al., 2012; Antonoudiou et al., 2020). This manipulation should consider the dynamic expression of NMDAr subtypes during neurodevelopment, across brain regions (Monyer et al., 1994; Murillo et al., 2021) and across neuronal types (von Engelhardt al., 2015).

To conclude, we showed that NMDAr blockade by MK801 induced positive and cognitive symptoms, altering the relationship between oscillations and locomotion and impairing theta/gamma co-modulation and its relationship with spatial working memory performance. We also found that changes in oscillatory activity were brain area specific. NMDAr's effect on different neuronal populations, and their specific roles in different brain areas, might explain the heterogeneity of the changes we observed under MK801. Further investigating how aberrant oscillatory activity, other neuronal populations, and different NMDAr subtypes contribute to SCZ's behavioral and cognitive deficits is necessary to understand the mechanisms underlying this disorder.

Author contributions

JRBM and RR designed the experiments. JRBM and PA implemented the experiments, developed and implemented the analysis toolbox. JRBM, RR, and PA discussed and interpreted the results. VB and LM supported the project providing resources for its development and discussed the results. JBRM wrote the paper, and the manuscript was further reviewed and data discussed by RR and PA.

Acknowledgments

We would like to thank Laia Serratosa Capdevila for her editing assistance. We thank Liset Menéndez de La Prida for her comments and suggestions in the initial version of the manuscript. We want to thank the support provided by the members of Victor Borrell Lab. Also, we want to thank the technical support provided by the SEA-UMH.

Funding: This project was supported by the Spanish State Research Agency, “Ministerio de Ciencia, Innovación y Universidades” (RTI2018-097474-A-100) and "Effect of RO compounds on the electrophysiological coupling of hippocampal-prefrontal circuits". F. Hoffmann-La Roche Ltd. by obtained by JRBM.

VB was supported by grants from the European Research Council (309633) and the Spanish State Research Agency (PGC2018-102172-B-I00, as well as through the “Severo Ochoa” Programme for Centers of Excellence in R&D, ref. SEV-2017-0723).

References

Housh AA, Berkowitz LE, Ybarra I, Kim EU, Lee BR, Calton JL (2014) Impairment of the anterior thalamic head direction cell network following administration of the NMDA antagonist MK-801. Brain Res Bull 109:77–87

Abekawa T, Ito K, Nakagawa S, Koyama T (2007) Prenatal exposure to an NMDA receptor antagonist, MK-801 reduces density of parvalbumin-immunoreactive GABAergic neurons in the medial prefrontal cortex and enhances phencyclidine-induced hyperlocomotion but not behavioral sensitization to methamphetamine in postpubertal rats. Psychopharmacology (Berl) 192:303–316.

Adell A, Jiménez-Sánchez L, López-Gil X, Romón T (2012) Is the acute NMDA receptor hypofunction a valid model of schizophrenia? Schizophr Bull 38:9–14

Adhikari A, Topiwala MA, Gordon JA (2009) Synchronized activity between the ventral hippocampus and the medial prefrontal cortex during anxiety.

Adler CM, Goldberg TE, Malhotra AK, Pickar D, Breier A (1998) Effects of ketamine on thought disorder, working memory, and semantic memory in healthy volunteers. Biol Psychiatry 43:811–816.

Hoover WB, Vertes RP (2007) Anatomical analysis of afferent projections to the medial prefrontal cortex in the rat. Brain Struct Funct 212:149–179.

Antonoudiou P, Tan YL, Kontou G, Upton AL, Mann EO (2020) Parvalbumin and Somatostatin Interneurons Contribute to the Generation of Hippocampal Gamma Oscillations. J Neurosci 40:7668

Ban TA (2007) Fifty years chlorpromazine: A historical perspective. Neuropsychiatr Dis Treat 3:495–500

Belforte JE, Zsiros V, Sklar ER, Jiang Z, Yu G, Li Y, Quinlan EM, Nakazawa K (2010) Postnatal NMDA receptor ablation in corticolimbic interneurons confers schizophrenia-like phenotypes. Nat Neurosci 13:76–83.

Beneyto M, Meador-Woodruff JH (2008) Lamina-specific abnormalities of NMDA receptor-associated postsynaptic protein transcripts in the prefrontal cortex in schizophrenia and bipolar disorder. Neuropsychopharmacology 33:2175–2186

Bokil H, Andrews P, Kulkarni JE, Mehta S, Mitra P (2010) Chronux: A Platform for Analyzing Neural Signals. J Neurosci Methods 192:146

Bowie CR, Harvey PD (2006) Cognitive deficits and functional outcome in schizophrenia. Neuropsychiatr Dis Treat 2:531

Buzsáki G, Buhl DL, Harris KD, Csicsvari J, Czéh B, Morozov A (2003) Hippocampal network patterns of activity in the mouse. Neuroscience 116:201–211.

Buzsáki G, Watson BO (2012) Brain rhythms and neural syntax: Implications for efficient coding of cognitive content and neuropsychiatric disease. Dialogues Clin Neurosci 14:345–367

Bygrave AM, Masiulis S, Nicholson E, Berkemann M, Barkus C, Sprengel R, Harrison PJ, Kullmann DM, Bannerman DM, Kätzel D (2016) Knockout of NMDA-receptors from parvalbumin interneurons sensitizes to schizophrenia-related deficits induced by MK-801. Transl Psychiatry

Callicott JH, Bertolino A, Mattay VS, Langheim FJP, Duyn J, Coppola R, Goldberg TE, Weinberger DR (2000) Physiological dysfunction of the dorsolateral prefrontal cortex in schizophrenia revisited. Cereb Cortex 10:1078–1092.

Carlén M, Meletis K, Siegle JH, Cardin JA, Futai K, Vierling-Claassen D, Rühlmann C, Jones SR, Deisseroth K, Sheng M, Moore CI, Tsai LH (2012) A critical role for NMDA receptors in parvalbumin interneurons for gamma rhythm induction and behavior. Mol Psychiatry 17:537–548.

Chen Z, Resnik E, McFarland JM, Sakmann B, Mehta MR (2011) Speed Controls the Amplitude and Timing of the Hippocampal Gamma Rhythm. PLoS One 6:e21408

Del Arco A, Segovia G, Mora F (2008) Blockade of NMDA receptors in the prefrontal cortex increases dopamine and acetylcholine release in the nucleus accumbens and motor activity. Psychopharmacology (Berl) 201:325–338.

Del Pino I, Brotons-Mas JR, Marques-Smith A, Marighetto A, Frick A, Marín O, Rico B (2017) Abnormal wiring of CCK^+basket cells disrupts spatial information coding. Nat Neurosci 20.

delPino I, García-Frigola C, Dehorter N, Brotons-Mas JR, Alvarez-Salvado E, MartínezdeLagrán M, Ciceri G, Gabaldón MV, Moratal D, Dierssen M, Canals S, Marín O, Rico B (2013) Erbb4 Deletion from Fast-Spiking Interneurons Causes Schizophrenia-like Phenotypes. Neuron 79:1152–1168

Eyjolfsson EM, Brenner E, Kondziella D, Sonnewald U (2006) Repeated injection of

MK801: An animal model of schizophrenia? Neurochem Int 48:541–546.

Hakami, T., Jones, N. C., Tolmacheva, E. A., Gaudias, J., Chaumont, J., Salzberg, M., O'Brien, T. J. & Pinault, D. (2009). NMDA Receptor Hypofunction Leads to Generalized and Persistent Aberrant gamma Oscillations Independent of Hyperlocomotion and the State of Consciousness. PLOS ONE, 4 (8), https://doi.org/10.1371/journal.pone.0006755.

Hargreaves EL, Côté D, Shapiro ML (1997) A dose of MK801 previously shown to impair spatial learning in the radial maze attenuates primed burst potentiation in the dentate gyrus of freely moving rats. Behav Neurosci 111:35–48

Hertzman M, Reba RC, Kotlyarov E V. (1990) Single photon emission computed tomography in phencyclidine and related drug abuse. Am J Psychiatry 147:255–256 Available at: https://pubmed.ncbi.nlm.nih.gov/2301671/

Homayoun H, Moghaddam B (2007) NMDA receptor hypofunction produces opposite effects on prefrontal cortex interneurons and pyramidal neurons. J Neurosci 27:11496–11500

Hudson MR, Sokolenko E, O’Brien TJ, Jones NC (2020) NMDA receptors on parvalbumin-positive interneurons and pyramidal neurons both contribute to MK-801 induced gamma oscillatory disturbances: Complex relationships with behaviour. Neurobiol Dis. 134:104625. doi: 10.1016/j.nbd.2019.104625

Huettner JE, Bean BP (1988) Block of N-methyl-D-aspartate-activated current by the anticonvulsant MK-801: Selective binding to open channels Proc Natl Acad Sci U S A. 1988 Feb;85(4):1307-11. doi: 10.1073/pnas.85.4.1307.

Ibarz JM, Foffani G, Cid E, Inostroza M, Prida LM de la (2010) Emergent Dynamics of Fast Ripples in the Epileptic Hippocampus. J Neurosci 30:16249–16261

Inostroza M, Brotons-Mas JR, Laurent F, Cid E, de la Prida LM (2013) Specific impairment of “What-Where-When” episodic-like memory in experimental models of temporal lobe epilepsy. J Neurosci 33:17749–17762.

von Engelhardt J, Bocklisch C, Tönges L, Herb A, Mishina M, Monyer H (2015) GluN2D-containing NMDA receptors-mediate synaptic currents in hippocampal interneurons and pyramidal cells in juvenile mice. Front Cell Neurosci

Jackson ME, Homayoun H, Moghaddam B (2004) NMDA receptor hypofunction produces concomitant firing rate potentiation and burst activity reduction in the prefrontal cortex. Proc Natl Acad Sci USA . 2004 Jun 1;101(22):8467-72. doi:

10.1073/pnas.030845510 [Accessed June 10, 2021].

James SL et al. (2018) Global, regional, and national incidence, prevalence, and years lived with disability for 354 Diseases and Injuries for 195 countries and territories, 1990-2017: A systematic analysis for the Global Burden of Disease Study 2017. Lancet 392:1789–1858.

Jodo E (2013) The role of the hippocampo-prefrontal cortex system in phencyclidine-induced psychosis: A model for schizophrenia. J Physiol Paris 107:434–440.

Jones MW, Wilson MA (2005) Theta rhythms coordinate hippocampal-prefrontal interactions in a spatial memory task. PLoS Biol 3:1–13

Kirkpatrick B, Fenton WS, Carpenter WT, Jr., Marder SR (2006) The NIMH-MATRICS Consensus Statement on Negative Symptoms. Schizophr Bull 32:214

Kiss T, Feng J, Hoffmann WE, Shaffer CL, Hajós M (2013) Rhythmic theta and delta activity of cortical and hippocampal neuronal networks in genetically or pharmacologically induced N-methyl-d-aspartate receptor hypofunction under urethane anesthesia. Neuroscience 237:255–267

Kittelberger K, Hur EE, Sazegar S, Keshavan V, Kocsis B (2012) Comparison of the effects of acute and chronic administration of ketamine on hippocampal oscillations: Relevance for the NMDA receptor hypofunction model of schizophrenia. Brain Struct Funct 217:395–409

Korotkova T, Fuchs EC, Ponomarenko A, von Engelhardt J, Monyer H (2010) NMDA Receptor Ablation on Parvalbumin-Positive Interneurons Impairs Hippocampal Synchrony, Spatial Representations, and Working Memory. Neuron 68:557–569.

Kramis R, Vanderwolf CH, Bland BH (1975) Two types of hippocampal rhythmical slow activity in both the rabbit and the rat: Relations to behavior and effects of atropine, diethyl ether, urethane, and pentobarbital. Exp Neurol 49:58–85.

Kristiansen L V., Beneyto M, Haroutunian V, Meador-Woodruff JH (2006) Changes in NMDA receptor subunits and interacting PSD proteins in dorsolateral prefrontal and anterior cingulate cortex indicate abnormal regional expression in schizophrenia. Mol Psychiatry 11:737–747.

Kropff E, Carmichael JE, Moser EI, Moser MB (2021) Frequency of theta rhythm is controlled by acceleration, but not speed, in running rats. Neuron 109:1029-1039.e8.

Lewis DA, Curley AA, Glausier JR, Volk DW (2012) Cortical parvalbumin interneurons and cognitive dysfunction in schizophrenia. Trends Neurosci 35:57–67

Long LL, Hinman JR, Chen CM, Escabi MA, Chrobak JJ (2014) Theta dynamics in rat: Speed and acceleration across the septotemporal axis. PLoS One 9

Lopez-Pigozzi D, Laurent F, Brotons-Mas JR, Valderrama M, Valero M, Fernandez-Lamo I, Cid E, Gomez-Dominguez D, Gall B, de la Prida LM (2016) Altered oscillatory dynamics of CA1 parvalbumin basket cells during theta-gamma rhythmopathies of temporal lobe epilepsy. eNeuro 3:1–20.

Malhotra AK, Pinals DA, Adler CM, Elman I, Clifton A, Pickar D, Breier A (1997) Ketamine-induced exacerbation of psychotic symptoms and cognitive impairment in neuroleptic-free schizophrenics. Neuropsychopharmacology 17:141–150.

Meltzer HY, Stahl SM (1976) the dopamine hypothesis of schizophreniaa review. Schizophr Bull. 1976;2(1):19-76. doi: 10.1093/schbul/2.1.19.

Mena A, Ruiz-Salas JC, Puentes A, Dorado I, Ruiz-Veguilla M, De la Casa LG (2016) Reduced prepulse inhibition as a biomarker of schizophrenia. Front Behav Neurosci 10:202

Miedel CJ, Patton JM, Miedel AN, Miedel ES, Levenson JM (2017) Assessment of Spontaneous Alternation, Novel Object Recognition and Limb Clasping in Transgenic Mouse Models of Amyloid-β and Tau Neuropathology. J Vis Exp:55523

Moghaddam B, Javitt D (2012) From revolution to evolution: The glutamate hypothesis of schizophrenia and its implication for treatment. Neuropsychopharmacology 37:4–15

Monyer H, Burnashev N, Laurie DJ, Sakmann B, Seeburg PH (1994) Developmental and regional expression in the rat brain and functional properties of four NMDA receptors. Neuron 12:529–540.

Murillo A, Navarro AI, Puelles E, Zhang Y, Petros TJ, Pérez-Otaño I (2021) Temporal Dynamics and Neuronal Specificity of Grin3a Expression in the Mouse Forebrain. Cereb Cortex 31:1914–1926

Murueta-Goyena Larrañaga A., Odrioizola A.B., Gargiulo P.Á., Lafuente Sánchez J.V. (2017) Neuropathological Background of MK-801 for Inducing Murine Model of Schizophrenia. In: Gargiulo P., Mesones-Arroyo H. (eds) Psychiatry and Neuroscience Update - Vol. II. Springer, Cham. https://doi.org/10.1007/978-3-319-

53126-7_25

Navas-Olive A, Valero M, Jurado-Parras T, de Salas-Quiroga A, Averkin RG, Gambino G, Cid E, de la Prida LM (2020) Multimodal determinants of phase-locked dynamics across deep-superficial hippocampal sublayers during theta oscillations. Nat Commun

Olney JW, Newcomer JW, Farber NB (1999) NMDA receptor hypofunction model of schizophrenia. J Psychiatr Res 33:523–533.

Olszewski M, Dolowa W, Matulewicz P, Kasicki S, Hunt MJ (2013) NMDA receptor antagonist-enhanced high frequency oscillations: Are they generated broadly or regionally specific? Eur Neuropsychopharmacol 23:1795–1805

Owen MJ, Sawa A, Mortensen PB (2016) Schizophrenia. Lancet 388:86–97

Richard GR, Titiz A, Tyler A, Holmes GL, Scott RC, Lenck-Santini P-P (2013.) Speed Modulation of Hippocampal Theta Frequency Correlates With Spatial Memory Performance. Hippocampus. 2013 Dec;23(12):1269-79. doi: 10.1002/hipo.22164. Epub 2013 Aug 5.

Royer S, Zemelman B V, Losonczy A, Kim J, Chance F, Magee JC, Buzsáki G (2012) Control of timing, rate and bursts of hippocampal place cells by dendritic and somatic inhibition. Nat Neurosci 15:769

Sigurdsson T, Duvarci S (2016) Hippocampal-prefrontal interactions in cognition, behavior and psychiatric disease. Front Syst Neurosci 9

Sigurdsson T, Stark KL, Karayiorgou M, Gogos JA, Gordon JA (2010) Impaired hippocampal-prefrontal synchrony in a genetic mouse model of schizophrenia. Nature 464:763–767.

Tamura M, Spellman TJ, Rosen AM, Gogos JA, Gordon JA (2017) Hippocampal-prefrontal theta-gamma coupling during performance of a spatial working memory task. Nat Commun 8.

Terrazas A, Krause M, Lipa P, Gothard KM, Barnes CA, McNaughton BL (2005) Self-Motion and the Hippocampal Spatial Metric. J Neurosci 25:8085–8096

Uhlhaas PJ, Singer W (2010) Abnormal neural oscillations and synchrony in schizophrenia. Nat Rev Neurosci 11:100–113

Valero M, de la Prida LM (2018) The hippocampus in depth: a sublayer-specific perspective of entorhinal–hippocampal function. Curr Opin Neurobiol 52:107–114.

Vollenweider FX, Vontobel P, Øye I, Hell D, Leenders KL (2000) Effects of (S)-ketamine on striatal dopamine: A [11C]raclopride PET study of a model psychosis in humans. J Psychiatr Res 34:35–43.

Wędzony K, Klimek V, Goembiowska K (1993) MK-801 elevates the etracellular concentration of dopamine in the rat prefrontal cortex and increases the density of striatal dopamine D1 receptors. Brain Res 622:325–329.

Weickert CS, Fung SJ, Catts VS, Schofield PR, Allen KM, Moore LT, Newell KA, Pellen D, Huang XF, Catts S V., Weickert TW (2013) Molecular evidence of N-methyl-D-aspartate receptor hypofunction in schizophrenia. Mol Psychiatry 18:1185–1192

Weickert TW, Goldberg TE, Gold JM, Bigelow LB, Egan MF, Weinberger DR (2000) Cognitive impairments in patients with schizophrenia displaying preserved and compromised intellect. Arch Gen Psychiatry 57:907–913.

Whishaw IQ, Vanderwolf CH (1973) Hippocampal EEG and behavior: Change in amplitude and frequency of RSA (Theta rhythm) associated with spontaneous and learned movement patterns in rats and cats. Behav Biol 8:461–484.

Young CK, Ruan M, McNaughton N (2020) Speed modulation of hippocampal theta frequency and power predicts water maze learning. bioRxiv:2020.03.31.016907 Available at: https://www.biorxiv.org/content/10.1101/2020.03.31.016907v1 [Accessed July 8, 2021].